water

MDPI

Article

Application of GIS-Interval Rough AHP Methodology for Flood Hazard Mapping in Urban Areas

Ljubomir Gigović [1,*], Dragan Pamučar [2], Zoran Bajić [3] and Siniša Drobnjak [4]

[1] Department of Geography, University of Defence, 11000 Belgrade, Serbia
[2] Department of Logistics, University of Defence, 11000 Belgrade, Serbia; dpamucar@gmail.com
[3] Department of Military-Chemical Engineering, University of Defence, 11000 Belgrade, Serbia; zoran.bajic@va.mod.gov.rs
[4] Military Geographical Institute, 11000 Belgrade, Serbia; sdrobnjak81@gmail.com
* Correspondence: gigoviclj@gmail.com; Tel.: +381-113603261

Academic Editors: Giuseppe Tito Aronica and Bruno Merz
Received: 26 February 2017; Accepted: 18 May 2017; Published: 24 May 2017

Abstract: Floods are natural disasters with significant socio-economic consequences. Urban areas with uncontrolled urban development, rapid population growth, an unregulated municipal system and an unplanned change of land use belong to the highly sensitive areas where floods cause devastating economic and social losses. The aim of this paper is to present a reliable GIS multi-criteria methodology for hazard zones' mapping of flood-prone areas in urban areas. The proposed methodology is based on the combined application of geographical information systems (GIS) and multi-criteria decision analysis (MCDA). The methodology considers six factors that are relevant to the hazard of flooding in urban areas: the height, slope, distance to the sewage network, the distance from the water surface, the water table and land use. The expert evaluation takes into account the nature and severity of observed criteria, and it is tested using three scenarios: the modalities of the analytic hierarchy process (AHP). The first of them uses a new approach to the exploitation of uncertainty in the application of the AHP technique, the interval rough numbers (IR'AHP). The second one uses the fuzzy technique for the exploitation of uncertainty with the AHP method (F'AHP), and the third scenario contemplates the use of the traditional (crisp) AHP method. The proposed methodology is demonstrated in Palilula Municipality, Belgrade, Serbia. In the last few decades, Palilula Municipality has been repeatedly devastated by extreme flood events. These floods severely affected the transportation networks and other infrastructure. Historical flood inundation data have been used in the validation process. The final urban flood hazard map proves a satisfactory agreement between the flood hazard zones and the spatial distribution of historical floods that happened in the last 58 years. The results indicate that the scenario in which the IR'AHP methodology is used provides the highest level of compatibility with historical data on floods. The produced map showed that the areas of very high flood hazard are located on the left Danube River bank. These areas are characterized by lowland morphology, gentle slope, sewage network, expansion of impermeable locations and intense urbanization. The proposed GIS-IR'AHP methodology and the results of this study provide a good basis for developing a system of flood hazard management in urban areas and can be successfully used for spatial city development policy.

Keywords: GIS; multi-criteria decision-making; flood hazard mapping; interval rough numbers

1. Introduction

Floods fall into the most serious natural disasters in the world that endanger more lives and cause more property damage than any other natural phenomenon [1–5]. Human activities, such as the

growth of settlements and economic assets in flooding areas and the reduction of the area for natural water retention as a result of land use and climate change, contribute to increasing the probability of the adverse impacts of floods.

Due to the absolute and relative population growth of urban areas, cities are physically wider, which means the expanding residential zone, the business, commercial and industrial areas and the road and railway network in the natural and agricultural land around cities. It usually involves the removal or reduction of vegetation and construction of impervious surfaces in the form of buildings, sidewalks, parking lots and roads. The negative effect of urbanization is two-fold: on the one hand, it accumulates objects threatened by flooding, while on the other hand, narrowing the watercourse profile and reducing the throughput of land. The spread of impervious surfaces is the main driver of hydrological change and leads to an increase and acceleration of runoff storm water [6–10]. In underdeveloped areas, the development of cities and the changes that this development causes, usually are not accompanied by the construction of an adequate drainage system for the atmospheric water management. The classical approach based on the collection of rain water from the urban area sewage system and taking it through the fastest route to the closest recipient has been used instead. Most often, this approach results in inefficient solutions for the removal of atmospheric water, leading to increasingly frequent flooding. To overcome such a difficult situation, it is necessary to establish a systematic approach in order to define flood areas in urban zones as soon as possible [11].

Risk reduction and flood management in urban areas inhabited with a large population have multiple significances. In addition to reducing material and human losses, they reduce the uncontrolled contamination with pollutants of known or unknown origin in the urban environment, but also create conditions for optimal land use. Contemporary trends of integrated water management and planning in urban environments include adequate risk assessment of their appearance and implementation of a number of technical and preventive measures that enable the control of the movement of rainwater and waste water in all projected hydrological regimes and their subsequent draining through the drain and sewage system. Flood management cannot become technically controllable without a proper assessment of flood hazard mapping and flood hazard.

Flood mapping is a crucial element of flood risk management. Directive 2007/60/EC on the assessment and management of flood risks will require Member States to prepare two types of maps by 2013 [12]:

Flood hazard maps, showing the extent and expected water depths/levels of an area flooded in three scenarios, a low probability scenario or extreme events, in a medium probability scenario (at least with a return period of 100 years) and, if appropriate, a high probability scenario.

Flood risk maps shall also be prepared for the areas flooded under these scenarios showing potential population, economic activities and the environment at potential risk from flooding and other information that Member States may find useful to include, for instance other sources of pollution. Accordingly, the first step is the hazard mapping, containing information on the flooding areas, which is the subject of the work.

In addition to the assessment, the flood hazard maps are useful tools for spatial planning and development of the city, especially in the area where it is necessary to identify infrastructure guidelines for the construction of a sewage drainage system and to determine the extent of the strict construction of new settlements [13].

Nowadays, the risk analysis of natural disasters is unimaginable without the digital backing and support of geographic information systems (GIS). Natural disasters are multidimensional phenomena with a spatial dimension, which makes GIS very applicative for such analysis [14–23]. Geographic information systems are suitable for this type of study because the powerful geostatistical tool can effectively manage large volumes of spatial data, and many studies dealing with flood risks and flood modeling effectively use GIS [24–26].

However, the application of GIS in the process of decision-making has certain shortcomings, which are reflected in the inability of multiple criteria analysis, which affects the decision-making.

In order to enable multi-criteria decision-making and presentation of the results in the area using GIS, it is necessary to combine tools for multi-criteria decision analysis (MCDA) with GIS. The application of MCDA in the GIS environment is currently a fundamental tool to solve problems in many areas, because it allows greater flexibility and accuracy in decision-making [27–32].

Over the last few decades, the combination of GIS and MCDA has been successful, and in a number of studies, it is often used in the risk assessment and generation of flood risk maps [8,15,33–40]. The researchers have used different methods and models for mapping of natural hazards using the GIS techniques [41–45]. A number of studies show that AHP in the GIS environment is the most popular and powerful method for generating flood hazard maps, with a good degree of accuracy, and it is suitable for other hazard studies. Many authors describe AHP as a user-friendly, cost-effective and convenient method for flood risk assessment [9,35,46–56].

This paper investigates the use of the GIS-MCDA methodology for assessing flood hazard in urban areas. The methodology considers six criteria: height, slope, distance to the sewers, distance from the river, the water table and land use. The goal of implementing the GIS interval rough numbers AHP (IR'AHP) methodology is the mapping of flood hazards. This map is the first step in the development plans of flood risk management [57].

Criteria weights in GIS IR'AHP methodology were determined by the IR'AHP technique, which represents a new approach in this field. As one of the most popular methods of multi-criteria decision-making, AHP has been widely used in a variety of policy issues, particularly in the problem of solving criteria weights [58]. It provides the ability to measure the consistency of decision-makers (DM) preferences in group decision-making and allows the manipulation of qualitative and quantitative criteria. The final decision when using the AHP method is made on the basis of subjective evaluations of DM [59]. Because of the subjectivity and ambiguity that occur in group decision-making, this paper used the interval rough numbers, combined with the AHP method in order to exploit that subjectivity. After determining the weight coefficients applying criteria IR'AHP techniques, a comparison of the results (weights) obtained that way and using fuzzy AHP (F'AHP) and the traditional (crisp) AHP technique was made. The process of comparing results or the comparison of the weight criteria included three scenario modalities. The first scenario involved the use of a new approach, or IR'AHP technique. The second and third scenario implied the application of the F'AHP and traditional (crisp) AHP techniques, respectively. After the validation, using historical events with the generated flood maps of the flood hazard in scenarios, the F'AHP technique that uses interval rough numbers is proven to be the most accurate.

It turned out that the IR'AHP methodology objectively considers uncertainties that occur in group decision-making, which is one of the contributions of this work. Another contribution of this work is the fact that the IR'AHP GIS-MCDA methodology rationally exploits uncertainty in group decision-making and objectively brings out flood hazard maps. The third contribution of this paper is the improvement of the methodology for evaluating the hazard of flooding in urban areas through a new approach to the treatment of uncertainty. The proposed methodology allows the evaluation of alternatives in spite of uncertainties in the process of decision-making and the lack of quantitative information. The results show a significant advantage of the IR'AHP GIS-MCDA methodology in comparison to those who have used the traditional and fuzzy AHP methodology with GIS for the evaluation of the risk of flooding in urban areas [46–56]. According to the authors' knowledge, the methodology presented in this paper represents a new approach to the GIS MCDA literature that contributes to the improvement of MCDA techniques.

The aim of this paper is to present a reliable GIS multi-criteria methodology for hazard zones' mapping of flood-prone areas in urban areas. The paper is organized into six sections. In the Introduction section, the importance of the problem of the increasingly frequent occurrence of floods in urban areas is defined and highlighted, thus giving an overview of the GIS and MCDA-AHP methodology relevant to the analysis and preparation of flood hazard maps. The second section contains a brief description of the geographical urban area of Palilula in Belgrade, Serbia.

The methodology and the description of the GIS-IR'AHP methodology phases are presented in the third section of the paper. The fourth section covers the estimation of flood-prone areas in Palilula municipality. The fifth section covers the discussion and the results' validation. Concluding considerations are given in the last, sixth section.

2. Study Area

The study area includes the urban community of Palilula, located in the northern part of the city of Belgrade in Serbia. Palilula extends to 71 km^2 and lies on the alluvial banks of the Danube River, of which 11.9 km^2 is covered by water surfaces (Figure 1). A total of 32% of the municipality is highly urbanized. On the non-urban part of it, mostly on the left river bank, the land is flat, swampy and marshy. The area of Palilula is characterized by the highest groundwater level in Belgrade. According to the last census of 2011, the population of the Palilula urban community is 110,637 persons, and it is constantly increasing due to the present process of urbanization [60].

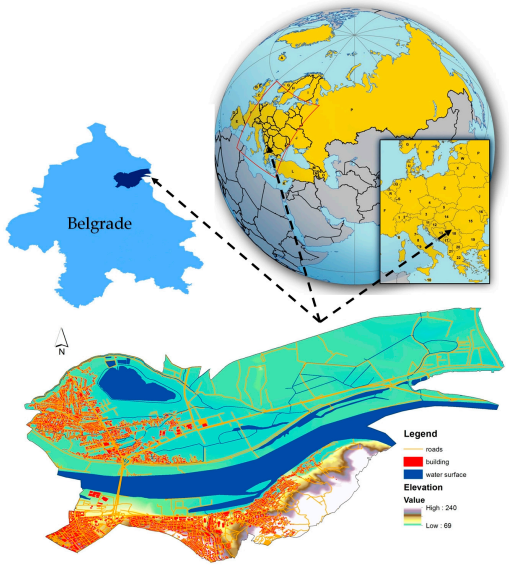

Figure 1. Location of the study area.

These changes negatively affect the expansion of impermeable surfaces and cause an increase and acceleration of storm water runoff. The expansion of drains and the sewage network is not adequately monitored with the urbanization and population growth, but the system for collecting rainwater from the area and its transfer mostly relies on the existing sewer system that does not have sufficient capacity and is obsolete. Recipients of rainfall water are existing melioration channels, inadequately maintained and with suspicious functionality due to the urbanization. When the rain is of high intensity for a period of 24 h, the existing systems are unable to absorb rainfall, leading to their spillover phenomena, causing extensive damage of floods. A particular problem of Palilula, especially in areas on the left bank of the Danube, is unplanned construction, a high level of groundwater and unsatisfactory sanitary conditions of life of the population in most parts of the municipality. For these reasons, frequent floods, in addition to considerable material damage, contamination with pollutants, disgorging sewage and septic tanks cause environmental disaster and endanger the health of the population. Remediation of this problem is an urgent problem of the city administration.

The mean annual precipitation for the period of 1851–2015 is approximately 710 mm (Figure 2). The majority of rains fall in June and May. In June, there is 12–13% of the total annual precipitation sum [61].

Data from the Belgrade meteorological station show several average annual precipitations for different periods (Figure 2). It can be seen from the total annual precipitation that for a total of four

out of the five analyzed periods, the total annual amount of precipitation was about 700 mm, while in the period of 1901–1930, there was a very strong minimum. However, when it comes to the trend, we cannot talk about some significant changes over long periods of time.

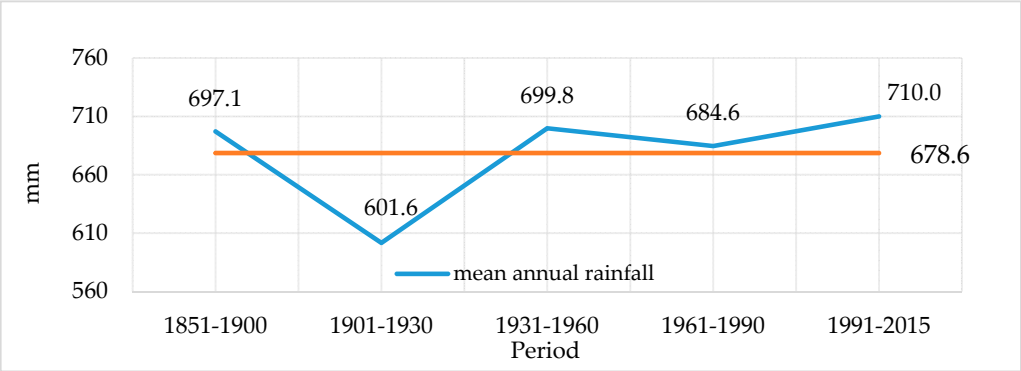

Figure 2. Average annual value of rainfall for the Palilula area.

Lately, there have been more extreme rainfalls, thus influencing the character of fluvial floods in urban areas. The occurrence of fluvial floods in the Palilula area is in a causal relation with the occurrence of extreme rain events. Therefore, predicting such phenomena is of great importance. Till now, several authors have contributed to this matter. Đorđević [62] analyzed trends for the annual and seasonal rainfalls and temperatures along with the extremity indexes of these parameters for Belgrade in the period of 1888–2006. It is found that the annual rainfalls increase while the number of rainy days is lessened for all seasons, except summer. An increase in the frequency of extreme rainfall events is also found, which is of particular importance for the occurrence of floods. Unkašević et al. [63], in a statistical analysis of monthly rainfall and maximum daily precipitation for Belgrade in the period of 1888–1995, indicate the importance of climate changes. According to them, the most common maximum daily precipitation events are associated with more frequent cold fronts followed by torrential rain and stormy weather and cyclones over the Eastern Mediterranean with centers in the southwest coast of the Black Sea. Precisely as a result of the formation of the spatial cyclone, which is shifted over the Adriatic to the Balkans, in the period from 14 to 16 May 2014, the largest flooding in the Palilula area is recorded when in the two days, the measured precipitation was 152.3 mm [62].

Relying on those studies, the increase of the extreme precipitation frequency, and thus, the number of floods with catastrophic consequences, is expected in the future in the area of Belgrade and Palilula. In the prevention of damage caused by floods, it is necessary to know the maximum range of this extreme event. It is of particular importance in the shortest possible time to define the boundaries of flooded areas. The first step is the mapping of flood hazards for Palilula.

3. Methodology

3.1. Methodological Background

The methodological hierarchy in this paper is based on the GIS-multi-criteria decision analysis (MCDA) structure. This approach uses the capabilities of GIS in the management of geospatial data and the flexibility MCDA to combine factual information (e.g., land use, slope, drainage system, etc.) with value-based information (e.g., expert opinion, standards, surveys, etc.). From a methodological point of view, the proposed defined flood zones in the municipality of Palilula include the following main steps (Figure 3).

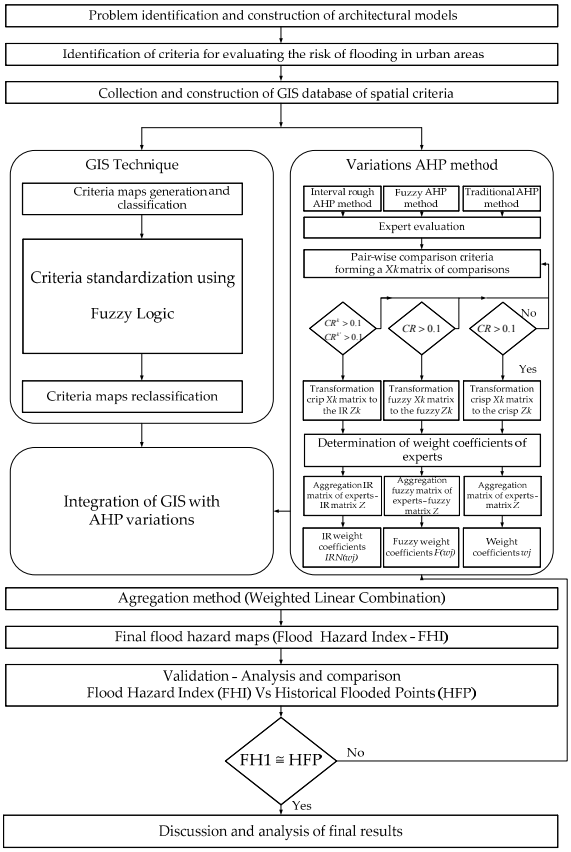

Figure 3. Flowchart of the applied methodology.

3.2. Interval Rough Numbers

Since the expansion of the rough numbers is a new methodology, the next section will illustrate the basic ideas and preferences of interval rough numbers (*IRN*). The process of group decision-making is accompanied by a large amount of uncertainty and subjectivity, and decision-makers often have a dilemma when allocating the value of certain attributes' decision. These uncertainties and ambiguities are commonly exploited with the application of interval numbers [64,65], fuzzy sets [66–68], rough numbers [58,59,69,70], gray theory [71–73] and by applying other approaches. The basic idea of applying algorithms to make decisions that are based on interval access (interval numbers, gray theory, and so on) involves the use of interval numbers presenting attribute value decisions. However, the boundaries of the interval in interval numbers are very difficult to determine and are based on the experience and intuition of decision-makers.

A large number of authors uses the process of the multi-criteria decision-making benefits of fuzzy sets to exploit ambiguity as their default [66] or through the different types of fuzzy theory extensions [74–79]. In addition, fuzzy sets are a very powerful tool for representing imprecision; the choice of membership functions of fuzzy sets is based on subjectivity and shall be based on experience and intuition [80]. In the process of decision-making, the intention of interval fuzzy techniques is that the crisp numbers were transformed into fuzzy numbers using the membership functions, which show uncertainties that exist in the real environment. In contrast to the theory of fuzzy sets whose application requires the definition of partial membership functions without clear boundaries set, rough set theory uses the border area set to express concerns. Unlike the fuzzy theory and probability theory in which the degree of uncertainty is defined based on assumptions, the theory of rough sets [81,82] determines the ambiguity on the basis of approximations, which is the basic concept of rough sets.

In theory, rough sets are used exclusively with in-house knowledge and operational data, and there is no need to rely on model assumptions. In other words, for the application of rough sets, instead of various additional/external parameters, the structure of the data provided is used exclusively [83]. In rough sets, the measurement of uncertainty is based on the uncertainty that is already contained in the data [84]. Thus, we come to objective indicators contained in the data.

In this paper, a new approach in the theory of rough sets is applied for the measurement of uncertainty that is already contained in the data, an approach that is based on intermittent rough numbers. Since this is a new approach, the authors found in the literature only a few papers that deal with the application of interval rough numbers in the field of multi-criteria decision-making [80]. One of the goals of this paper is to initiate other authors for the wider application of *IRN* in MCDM, since the *IRN* benefits outlined in this paper represent a logical motive for their wider application.

Suppose there is a set of k classes that represents DM preferences, $R = (J_1, J_2, ..., J_k)$, on the condition that they belong to a series, which satisfies the requirement that the $J_1 < J_2 <, ..., < J_k$ and second set of m classes that also represents DM preferences, $R^* = (I_1, I_2, ..., I_k)$. All objects are defined in the universe and connected with the DM preferences. In R^*, each object class is presented in the interval $I_i = \{I_{li}, I_{ui}\}$, where the next condition is satisfied $I_{li} \leq I_{ui}$ $(1 \leq i \leq m)$, and also $I_{li}, I_{ui} \in R$. Then, I_{li} denotes lower interval limit, while I_{ui} denotes upper interval limit of the i-th object class. If both boundaries of a class of objects (upper and lower limit) are listed in a way that is $I^*_{l1} < I^*_{l2} <, ..., < I^*_{lj}, I^*_{u1} < I^*_{u2} <, ..., < I^*_{uk}$ $(1 \leq j, k \leq m)$, respectively, then, we can define two new sets containing the lower class of objects $R^*_l = (I^*_{l1}, I^*_{l2}, ..., I^*_{lj})$ and the upper class of objects $R^*_u = (I^*_{u1}, I^*_{u2}, ..., I^*_{uk})$, respectively. Then, for any class of objects $I^*_{li} \in R$ $(1 \leq i \leq j)$ and $I^*_{ui} \in R$ $(1 \leq i \leq k)$, we can define the lower approximations of I^*_{li} and I^*_{ui} as follows:

$$\underline{Apr}(I^*_{li}) = \cup\{Y \in U/R^*_l(Y) \leq I^*_{li}\} \tag{1}$$

$$\underline{Apr}(I^*_{ui}) = \cup\{Y \in U/R^*_u(Y) \leq I^*_{ui}\} \tag{2}$$

The upper approximations of I^*_{li} and I^*_{ui} are defined in the next equations:

$$\overline{Apr}(I^*_{li}) = \cup\{Y \in U/R^*_l(Y) \geq I^*_{li}\} \tag{3}$$

$$\overline{Apr}(I^*_{ui}) = \cup\{Y \in U/R^*_u(Y) \geq I^*_{ui}\} \tag{4}$$

Both object classes (upper and lower I^*_{li} and I^*_{ui}) are defined with their lower limits $\underline{Lim}(I^*_{li})$ and $\underline{Lim}(I^*_{ui})$ and upper limits $\overline{Lim}(I^*_{li})$ and $\overline{Lim}(I^*_{ui})$, respectively.

$$\underline{Lim}(I^*_{li}) = \frac{1}{M_L}\sum R^*_l(Y)|Y \in \underline{Apr}(I^*_{li}) \tag{5}$$

$$\underline{Lim}(I^*_{ui}) = \frac{1}{M^*_L}\sum R^*_u(Y)|Y \in \underline{Apr}(I^*_{ui}) \tag{6}$$

where M_L and M^*_L represent the sum of objects that are contained in the lower approximation of a class of objects I^*_{li} and I^*_{ui}, respectively. Upper limits $\overline{Lim}(I^*_{li})$ and $\overline{Lim}(I^*_{ui})$ are defined with Equations (7) and (8).

$$\overline{Lim}(I^*_{li}) = \frac{1}{M_U}\sum R^*_l(Y)|Y \in \overline{Apr}(I^*_{li}) \tag{7}$$

$$\overline{Lim}(I^*_{ui}) = \frac{1}{M^*_U}\sum R^*_u(Y)|Y \in \overline{Apr}(I^*_{ui}) \tag{8}$$

where M_U and M^*_U represent the sum of objects that are contained in the upper approximation of a class of objects I^*_{li} and I^*_{ui}, respectively.

The rough boundary interval for the lower object class I_{li}^* is represented as $RB(I_{li}^*)$ and indicates the interval between the lower and upper limit:

$$RB(I_{li}^*) = \overline{Lim}(I_{li}^*) - \underline{Lim}(I_{li}^*) \tag{9}$$

while for the upper class of objects, the rough boundary interval I_{ui}^* is calculated as:

$$RB(I_{ui}^*) = \overline{Lim}(I_{ui}^*) - \underline{Lim}(I_{ui}^*) \tag{10}$$

Then, uncertain object classes I_{li}^* and I_{ui}^* can be shown by their lower and upper limit.

$$RN(I_{li}^*) = \left[\overline{Lim}(I_{li}^*), \underline{Lim}(I_{li}^*) \right] \tag{11}$$

$$RN(I_{ui}^*) = \left[\overline{Lim}(I_{ui}^*), \underline{Lim}(I_{ui}^*) \right] \tag{12}$$

As is seen, each class of objects is defined by its lower and upper limits, which make up an interval rough number, which is defined as:

$$IRN(I_i^*) = [RN(I_{li}^*), RN(I_{ui}^*)] \tag{13}$$

Interval rough numbers characterize specific arithmetic operations, which differ from the arithmetic operations with the classic rough numbers that are shown in Appendix A.

3.3. IR'AHP Mathematical Model

The next section describes the mathematical formulation of IR'AHP model. The IR'AHP model generally involves the implementation of the traditional AHP model [85,86]. The IR'AHP model allows decision-makers, if there are fluctuations in the comparison in pairs criteria, to make the comparisons matrix, enrolling two values from the Saaty scale on which the decision-maker is ambiguous. Therefore, we get the comparisons matrix in pairs that contain uncertainty that existed for the expert evaluation criteria. In a further implementation of the method, the uncertainty of the IR'AHP model is used to create interval rough numbers, Expressions (1)–(13). The algorithm of the IR'AHP model is implemented through five steps, which are presented in the following:

Step 1. Establishing a hierarchical structure of evaluation criteria: A group of experts is formed who carry out the selection criteria and define a problem hierarchy with global goals at the upper and at the lower level criteria.

Step 2. Filling a matrix to compare evaluation criteria in pairs: Members of the group of experts compare in pairs the evaluation criteria in order to define the criteria weights. Comparison in pairs is done using the Saaty ninth degree linguistic scale [86]. Each e-th expert presents his/her comparisons by using matrix:

$$Z_k = \begin{bmatrix} 1 & x_{12}^e; x_{12}^{e\prime} & \cdots & x_{1n}^e; x_{1n}^{e\prime} \\ x_{21}^e; x_{21}^{e\prime} & 1 & \cdots & x_{2n}^e; x_{2n}^{e\prime} \\ \vdots & \vdots & \ddots & \vdots \\ x_{n1}^e; x_{n1}^{e\prime} & x_{n2}^e; x_{n2}^{e\prime} & \cdots & 1 \end{bmatrix}_{nxn} ; 1 \le i, j \le n; 1 \le e \le k \tag{14}$$

where x_{ij}^k and $x_{ij}^{k\prime}$ are phrases from Saaty ninth degree linguistic scale used by expert k to present his/her comparison in criteria pairs.

If expert k finds uncertainty while comparing pairs of criteria (i, j), or actually expert k cannot decide between two values from the Saaty ninth degree linguistic scale, then both values are named $(x_{ij}^k \neq x_{ij}^{k\prime})$. If there is no uncertainty, then an expert unambiguously selects one value. Then, into the matrix of the comparison criteria (Z_k), the same value (i, j) is entered,$x_{ij}^k = x_{ij}^{k\prime}$. For example, an expert

during the criterion comparison at the position (1,2) cannot decide between two linguistic values (e.g., 5 and 6), then at the position (1,2) in the matrix Z_k $x_{12}^{e} = 5$ and $x_{12}^{e\prime} = 6$ are entered.

Thus, the Z_1,Z_2,...,Z_e matrix is obtained with e experts giving their comparison in criteria pairs.

Step 3. Determination of experts' weight coefficients: For each comparison, matrix Z_k is determined by the consistency of experts' evaluation. Saaty [86] suggested the consistency ratio (CR) for the consistency check. The calculation of the degree of consistency is done in two steps. In the first step, the consistency index (CI) is calculated $CI = (\lambda_{\max} - n)/(n-1)$, where n is matrix rank and $\lambda_{\max}$ the maximum Eigen value of the comparison matrix.

The second step calculates CR as the ratio between CI and the random index (RI).

$$CR = \frac{CI}{RI} \tag{15}$$

The random index (RI) depends on matrix rank, and its values are calculated with the random generation of 500 matrices [80]; see Table 1.

Table 1. Random index (RI) value depending on the matrix rank.

n	**1**	**2**	**3**	**4**	**5**	**6**	**7**	**8**	**9**	**10**
RI	0.00	0.00	0.52	0.89	1.11	1.25	1.35	1.40	1.45	1.49

If the consistency ratio (CR) is less than or equal to 0.10, that proves that the expert was consistent and that there is no need to repeat the evaluations [85]. If the CR is higher than 0.10, the decision-maker should repeat (or modify) his/her evaluation in order to improve his/her own consistency.

As every expert in the matrix Z_k at (i,j) enters two values, two CRs are obtained for each expert, CRe and CRe'. Prior to determining the final value (CR_k), the values of CRe and CRe' must meet the following requirements CRe $\geq$ 0.1 and CRe' $\geq$ 0.1. The final CR is calculated as medium value $CR_k = (CR^k + CR^{k\prime})/2$.

Experts' weighted coefficients are obtained by normalizing the reciprocal value of the consistency ratio, Equations (16) and (17).

$$W_i = \frac{1}{CR_k} \tag{16}$$

where CR_k is C_r for expert e and W_{ke} the weight coefficient for expert e. Normalization of the experts' weight coefficient is carried out using the additive normalization.

$$w_{ik} = \frac{W_i}{\sum\limits_{i=1}^{k} W_i} \tag{17}$$

where W_i is the weight coefficient for expert e.

Step 4. Construction of the average interval rough comparison matrix: Using Matrix (14) from all k experts, two matrices of aggregated experts' sequences are obtained, X^{*L} and $X^{*'U}$.

$$X^{*L} = \begin{bmatrix} x_{11}^{1L}, x_{11}^{2L}, \ldots, x_{11}^{kL} & x_{12}^{1L}; x_{12}^{2L}; \ldots; x_{12}^{kL}, & \ldots, & x_{1n}^{1L}; x_{1n}^{2L}, \ldots, x_{1n}^{kL} \\ x_{21}^{1L}, x_{21}^{2L}, \ldots, x_{21}^{kL} & x_{22}^{1L}; x_{22}^{2L}; \ldots; x_{22}^{kL}, & \ldots, & x_{2n}^{1L}; x_{2n}^{2L}, \ldots, x_{2n}^{kL} \\ \ldots & \ldots & \ldots & \ldots \\ x_{n1}^{1L}, x_{n1}^{2L}, \ldots, x_{n1}^{kL} & x_{n2}^{1L}; x_{n2}^{2L}; \ldots; x_{n2}^{kL}, & \ldots, & x_{nn}^{1L}; x_{nn}^{2L}, \ldots, x_{nn}^{kL} \end{bmatrix} \tag{18}$$

$$X^{*\prime U} = \begin{bmatrix} x_{11}^{1\prime U}, x_{11}^{2\prime U}, \ldots, x_{11}^{k\prime U} & x_{12}^{1\prime U}; x_{12}^{2\prime U}; \ldots; x_{12}^{k\prime U}, & \ldots, & x_{1n}^{1\prime U}; x_{1n}^{2\prime U}, \ldots, x_{1n}^{k\prime U} \\ x_{21}^{1\prime U}, x_{21}^{2\prime U}, \ldots, x_{21}^{k\prime U} & x_{22}^{1\prime U}; x_{22}^{2\prime U}; \ldots; x_{22}^{k\prime U}, & \ldots, & x_{2n}^{1\prime U}; x_{2n}^{2\prime U}, \ldots, x_{2n}^{k\prime U} \\ \ldots & \ldots & \ldots & \ldots \\ x_{n1}^{1\prime U}, x_{n1}^{2\prime U}, \ldots, x_{n1}^{k\prime U} & x_{n2}^{1\prime U}; x_{n2}^{2\prime U}; \ldots; x_{n2}^{k\prime U}, & \ldots, & x_{nn}^{1\prime U}; x_{nn}^{2\prime U}, \ldots, x_{nn}^{k\prime U} \end{bmatrix} \quad (19)$$

where $x_{ij}^{L} = \left\{x_{ij}^{1L}, x_{ij}^{2L}, \ldots, x_{ij}^{kL}\right\}$ and $x_{ij}^{\prime U} = \left\{x_{ij}^{1\prime U}, x_{ij}^{2\prime U}, \ldots, x_{ij}^{k\prime U}\right\}$ are sequences used to describe the relative significance of criterion i towards criterion j. Using Equations (1)–(13), each sequence x_{ij}^{k} and $x_{ij}^{k\prime}$ is transformed into rough sequence $RN\left(x_{ij}^{kL}\right) = \left[\underline{Lim}(x_{ij}^{kL}),\ \overline{Lim}(x_{ij}^{kL})\right]$ and $RN\left(x_{ij}^{k\prime U}\right) = \left[\underline{Lim}(x_{ij}^{k\prime U}),\ \overline{Lim}(x_{ij}^{k\prime U})\right]$, where $\underline{Lim}(x_{ij}^{kL})$ and $\underline{Lim}(x_{ij}^{k\prime U})$ are upper limits, while $\overline{Lim}(x_{ij}^{kL})$ and $\overline{Lim}(x_{ij}^{k\prime U})$ are upper limits of rough sequences $RN\left(x_{ij}^{kL}\right)$ and $RN\left(x_{ij}^{k\prime U}\right)$, respectively.

Such rough sequences are defined in the matrices (18) and (19). Thus, rough matrices X^{1L}, X^{2L}, ... , X^{mL} are obtained (where m is the number of experts) for the first rough sequence $RN\left(x_{ij}^{kL}\right)$ and $X^{1'U}$, $X^{2'U}$, ... , $X^{m'U}$ for the second rough sequence $RN\left(x_{ij}^{k\prime U}\right)$. For the first group of rough matrices X^{1L}, X^{2L}, ... , X^{mL} at (ij) rough sequence is obtained as follows:

$$RN\left(x_{ij}^{L}\right) = \left\{\left[\underline{Lim}(x_{ij}^{1L}),\ \overline{Lim}(x_{ij}^{1L})\right],\ \left[\underline{Lim}(x_{ij}^{2L}),\ \overline{Lim}(x_{ij}^{2L})\right], ..., \left[\underline{Lim}(x_{ij}^{mL}),\ \overline{Lim}(x_{ij}^{mL})\right]\right\} \quad (20)$$

In the same way, for the second group of rough matrices $X^{1'U}$, $X^{2'U}$, ... , $X^{m'U}$ at (ij) rough sequence is obtained $RN\left(x_{ij}^{\prime U}\right) = \left\{\left[\underline{Lim}(x_{ij}^{1\prime U}),\ \overline{Lim}(x_{ij}^{1\prime U})\right],\ \left[\underline{Lim}(x_{ij}^{2\prime U}),\ \overline{Lim}(x_{ij}^{2\prime U})\right], ..., \left[\underline{Lim}(x_{ij}^{m\prime U}),\ \overline{Lim}(x_{ij}^{m\prime U})\right]\right\}$.

Using Equations (21) and (22), average rough sequences are calculated:

$$RN(z_{ij}^{L}) = RN(x_{ij}^{1L}, x_{ij}^{2L}, ..., x_{ij}^{eL}) = \begin{cases} z_{ij}^{L} = \frac{1}{m}\sum_{e=1}^{m} x_{ij}^{eL} \\ z_{ij}^{U} = \frac{1}{m}\sum_{e=1}^{m} x_{ij}^{eU} \end{cases} \quad (21)$$

$$RN(z_{ij}^{\prime U}) = RN(x_{ij}^{1\prime U}, x_{ij}^{2\prime U}, ..., x_{ij}^{e\prime U}) = \begin{cases} z_{ij}^{\prime L} = \frac{1}{m}\sum_{e=1}^{m} x_{ij}^{e\prime L} \\ z_{ij}^{\prime U} = \frac{1}{m}\sum_{e=1}^{m} x_{ij}^{e\prime U} \end{cases} \quad (22)$$

where e is the e-th expert ($e = 1, 2, ..., m$) and $RN(z_{ij}^{L})$ and $RN(z_{ij}^{\prime U})$ are rough sequences representing the lower and upper limit of IRN, $IRN(z_{ij})$, $IRN(z_{ij}) = \left[RN(z_{ij}^{L}), RN(z_{ij}^{\prime U})\right]$.

Therefore, we get the average interval rough comparison matrix in pairs of evaluation criteria (Z):

$$Z = \begin{bmatrix} 1 & IRN(z_{12}) & \cdots & IRN(z_{1n}) \\ IRN(z_{21}) & 1 & \cdots & IRN(z_{2n}) \\ \vdots & \vdots & \ddots & \vdots \\ IRN(z_{n1}) & IRN(z_{n2}) & \cdots & 1 \end{bmatrix}_{nxn} \quad (23)$$

Step 5. Calculation of priority criteria vectors: The priority criteria vector represents an interval rough weighted coefficient $IRN(w_j)$, and it is determined for each n evaluation criteria. Interval rough weighted coefficient $IRN(w_j)$ is calculated using Equations (24)–(27). Using Equation (24), matrix Z elements are summed by columns.

$$IRN(a_{ij}^{\prime}) = \sum_{j=1}^{n} IRN(z_{ij}) = \left(\left[\sum_{j=1}^{n} z_{ij}^{L}, \sum_{j=1}^{n} z_{ij}^{U}\right], \left[\sum_{j=1}^{n} z_{ij}^{\prime L}, \sum_{j=1}^{n} z_{ij}^{\prime U}\right]\right) \quad (24)$$

Using Equation (25), the normalized matrix of weight coefficients W is calculated (26).

$$IRN(w_{ij}) = \left(\left[w_{ij}^{L}, w_{ij}^{U}\right], \left[w_{ij}^{\prime L}, w_{ij}^{\prime U}\right]\right) = \frac{IRN(z_{ij})}{\sum_{j=1}^{n} IRN(z_{ij})} = \frac{\left(\left[z_{ij}^{L}, z_{ij}^{U}\right], \left[z_{ij}^{\prime L}, z_{ij}^{\prime U}\right]\right)}{\left(\left[\sum_{j=1}^{n} z_{ij}^{L}, \sum_{j=1}^{n} z_{ij}^{U}\right], \left[\sum_{j=1}^{n} z_{ij}^{\prime L}, \sum_{j=1}^{n} z_{ij}^{\prime U}\right]\right)} \quad (25)$$

$$W = \begin{bmatrix} 1 & \left(\left[w_{12}^{L}, w_{12}^{U}\right], \left[w_{12}^{\prime L}, w_{12}^{\prime U}\right]\right) & \cdots & \left(\left[w_{1n}^{L}, w_{1n}^{U}\right], \left[w_{1n}^{\prime L}, w_{1n}^{\prime U}\right]\right) \\ \left(\left[w_{21}^{L}, w_{21}^{U}\right], \left[w_{21}^{\prime L}, w_{21}^{\prime U}\right]\right) & 1 & \cdots & \left(\left[w_{2n}^{L}, w_{2n}^{U}\right], \left[w_{2n}^{\prime L}, w_{2n}^{\prime U}\right]\right) \\ \vdots & \vdots & \ddots & \vdots \\ \left(\left[w_{n1}^{L}, w_{n1}^{U}\right], \left[w_{n1}^{\prime L}, w_{n1}^{\prime U}\right]\right) & \left(\left[w_{n2}^{L}, w_{n2}^{U}\right], \left[w_{n2}^{\prime L}, w_{n2}^{\prime U}\right]\right) & \cdots & 1 \end{bmatrix}_{nxn} \quad (26)$$

The final interval rough weight coefficients ($IRN(w_j)$) for the evaluation criteria are calculated using Equation (27).

$$IRN(w_j) = \left(\left[\sum_{i=1}^{n} w_{ij}^{L}, \sum_{i=1}^{n} w_{ij}^{U}\right], \left[\sum_{i=1}^{n} w_{ij}^{\prime L}, \sum_{i=1}^{n} w_{ij}^{\prime U}\right]\right)/n \quad (27)$$

where n is the number of evaluation criteria.

The values of the criteria weight coefficients are in the interval $IRN(w_j) = \left(\left[w_j^L, w_j^U\right], \left[w_j^{\prime L}, w_j^{\prime U}\right]\right)$ where the condition $0 \leq w_j^L \leq w_j^{\prime L} \leq w_j^U \leq w_j^{\prime U} \leq 1$ is fulfilled for each evaluation criteria $x_j \in X$. However, it is generally necessary that a sum of criteria weight coefficients is equal to one. In our case, since it is an interval rough weight coefficients criterion, using the expression (27), we obtain the weights $\sum_{j=1}^{n} w_j^L \leq 1$, $\sum_{j=1}^{n} w_j^{\prime L} \leq 1$, $\sum_{j=1}^{n} w_j^U \geq 1$ and $\sum_{j=1}^{n} w_j^{\prime U} \geq 1$. Thus, the condition is satisfied for the weight coefficients to be in the interval $w_i \in [0,1]$, $(i = 1, 2, ..., n)$.

4. Estimation of Flood-Prone Areas in Palilula Municipality

This section is divided into subsections. It provides a concise and precise description of the aim of this study. The aim is to propose a reliable GIS-MCDA methodology for the flood hazard mapping of urban areas, which could serve as a useful tool for preventing and reducing the hazard of flood damage for spatial planners to create spatial policies and systems for water management. In the criteria selection and zoning of flood hazard in the local community of Palilula, 10 experts participated. They have experience in the field of crisis management, hydrology, spatial planning and environmental protection. The experts' interviews are used to collect data that are further processed, and the aggregation of experts' opinions is executed.

4.1. Criteria Selection

The criteria selection for evaluating the hazard of floods is an important step of the analysis. It is essential to identify floods factors in order to create a reliable susceptibility to flood map [44]. Based on previous studies [10,55], experts' opinions and longer observations from the field, this study adopted six criteria that are an important cause of flooding in the local community of Palilula. The selected criteria with a brief description are as follows:

Elevation (C1): The study area is located on the alluvial plain of the Danube River and in the lowest part of Belgrade, in the relative range between 69 and 240 m above sea level. This criterion has a key role in controlling the movement of the overflow direction and in the depth of the water level [87]. Height values were obtained using a digital elevation model (DEM 25) made at the Military Geographical Institute in Belgrade.

Slope (C2) is an important indicator of a surface zones, which are highly prone to flooding [88,89]. Slope is a major factor in determining the rate and duration of water flow. On the flatter surface, water is moving more slowly, collects longer and accumulates so these areas are riskier with respect to the

occurrence of floods in relation to the steeper surfaces. Map inclination is prepared as percentages using the DEM of the studied area.

Distance from the drainage network (C3) has the greatest significance for the flood mapping in urban areas. As a result of rainfall overflow, areas near these channels during flooding in urban areas are the most affected [9]. In field studies, the sewerage network consists of channel wastewater systems, storm water systems and general system. Data for this criterion were obtained using the map from general solutions for the channeling of rainwater and wastewater from the General Urban Plan of Belgrade, which was established by the Town Planning Institute of Belgrade.

Distance from water surfaces (C4) has a significant impact on the spread and size of floods in the projected area [90]. River overflows are one of the main causes for the initiation of flooding. Often, flooding starts from the river or canal riverbed and expands in the region. The areas near bodies of water are very high-hazard areas for the occurrence of floods, and the effect of this criterion is reduced with increasing distance. The study area is dominated by the Danube as the largest body of water to which many open channels and streams gravitate.

Water table (C5) directly affects the infiltration capacity of the soil. In areas with low levels of groundwater, land area with the appearance of water is rapidly saturated, and the water is accumulated and spread to the surrounding area [9]. The data used in this study were obtained using the data perennial average groundwater level map from hydrology and geology "groundwater level", prepared by the Directorate for Building Land and Construction of Belgrade.

Land cover use (C6) is also one of the main factors that contributes to the occurrence of floods and has an important impact on runoff and the ability of soil to act as storage for water. Urban and industrial areas are mainly made of impervious surfaces (buildings, roads and parking lots), act as a barrier, reducing the infiltration capacity, retain water and are prone to floods. On the other side, the fields, pastures and forest vegetation are less prone to flooding [22,91]. The layer criteria for land cover of the studied area was prepared after integration of the Database Online Map Street within the ArcGIS software package [92]. For this study, land use is systematized into eight categories: urbanized areas, industrial areas, agricultural land, land covered with sparse vegetation, grassy areas and parks, forests, marshy areas and water surfaces.

The selected criteria in this paper are based on available data and are adapted to the objective natural and social conditions of the studied zone of Palilula. The applied methodology allows inclusion of other criteria that were not included in this study. This is primarily related to the flow accumulation, flow direction, wetness index, rainfall and the like. All newly-added criteria may have an additional role in the election of the best solution.

Once the criteria are defined, the next step of their evaluation is to build the spatial database and input this into GIS. In this way, each of the criteria has been converted in the form of spatially-defined layers of maps with the same grid cells size 15 m $\times$ 15 m, which are the units that are estimated. All of the processes of the transformation and GIS data modeling were performed using the integrated tool ESRI ArcGIS 10.2 software. Maps' criteria height and slope were obtained using the 3D Analyst algorithm based on DEM. Maps from the sewage network and water were obtained by the use of Radial Distance tools. Maps of the groundwater depth are obtained by georeferencing of the analogue map "groundwater level", drawn up by Directorate for building land and construction of Belgrade, while the land cover use map was obtained by importing OpenStreetMap (OSM) bases within the ArcGIS software environment.

4.2. GIS-MCDA

This phase involves the standardization, expert work, weighting, summary analysis, aggregation of all criteria to be considered in the decision-making process and their validation.

Given that the data were collected in different ways and have different formats, the first step is that all datasets have to be standardized and in units that can be compared. Based on the literature and the experience of experts, in this study, the fuzzy concept has been used to standardize the data criteria. The fuzzy logic concept is flexible and is suitable for data modeling in which there is no exact boundaries of the elements belonging to the set, determined as zero or one [64]. In such cases, the elements belonging to the set are defined on the basis of the degree of affiliation to a function (sigmoidal, J-shaped, linear or user-defined). Which membership functions will be used depends on the nature of the data and on the basis of the decisions and experience of experts.

In this case, with the criteria set whose elements have categorical values (land cover use), we used the discrete classification, in which experts directly determined the values of the elements of fuzzy sets. For other criteria, which are the values of the gradual change from one location to another, elements of the set are standardized using the fuzzy concept based on the linear membership function. A scale ranging from 0 to 1 bytes was used for fuzzification, where zero is the least hazard and one is the most dangerous element of the set value in relation to the likelihood of the occurrence of flooding (Table 2, Figure 4).

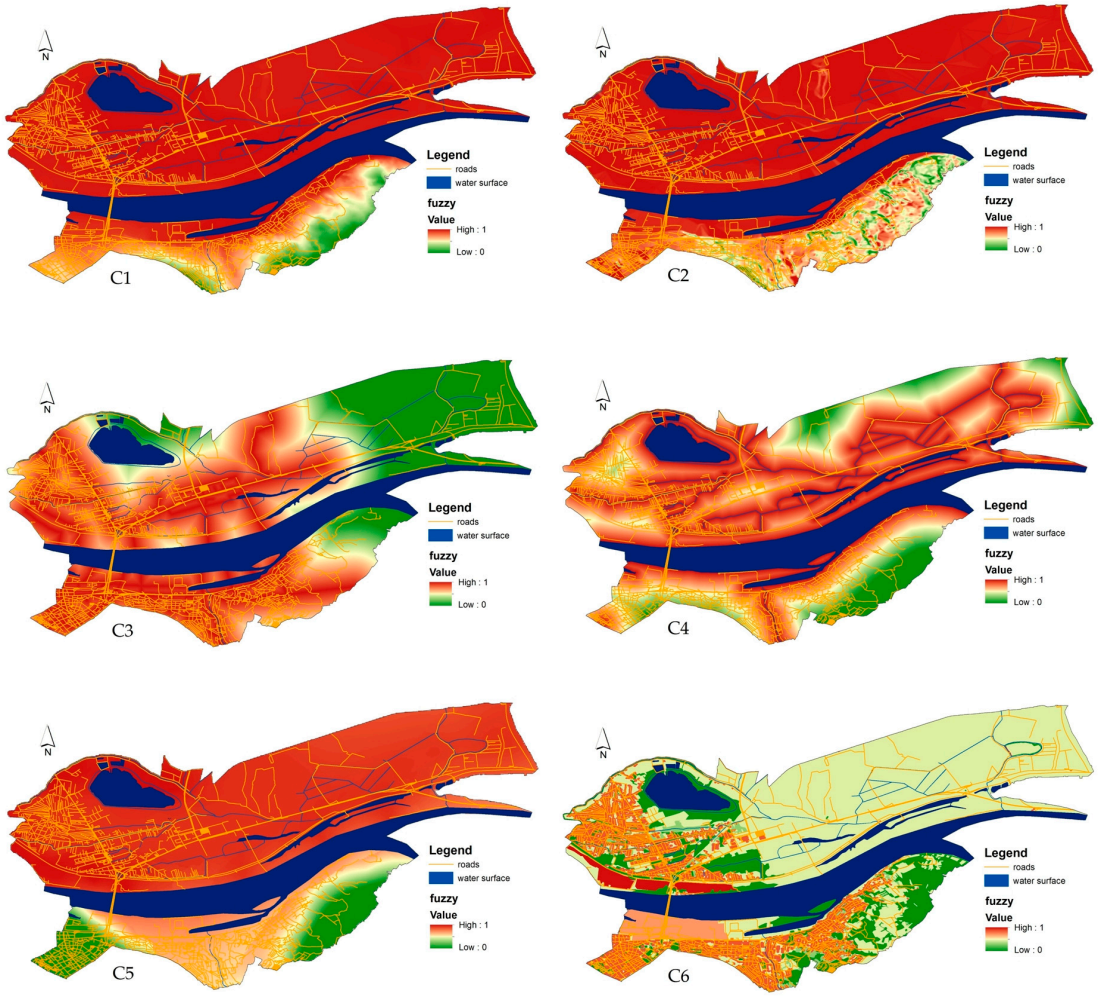

Figure 4. Maps of standardized criteria for the studied area.

Table 2. Fuzzy standardization of criteria.

Criteria	Fuzzy Membership Function	Control Points/ Value Points	Final Utility
Elevation (C1)	Linear monotonically decreasing	c = 50 m; d = 300 m	0–50 m equal to 1, 50–300 m between 1 and 0, more than 300 m equal to 0
Slope (C2)	Linear monotonically decreasing	c = 1°; d = 35°	0°–1° equal to 1, 1°–30° between 1 and 0, more than 35° equal to 0
Distance from drainage network (C3)	Linear monotonically decreasing	c = 100 m; d = 2000 m	0–100 m equal to 1, 100–2000 m between 1 and 0, more than 2000 m equal to 0
Distance from water surfaces (C4)	Linear monotonically decreasing	c = 100 m; d = 2000 m	0–100 m equal to 1, 100–2000 m between 1 and 0, more than 2000 m equal to 0
Water table(C5)	Linear monotonically decreasing	c = 100 cm; d = 5000 cm	0–100 cm equal to 1, 100–4000 cm between 1 and 0, more than 5000 cm equal to 0
Land cover use (C6)	Discrete categorical data	Water areas equal 1; wetlands equal 0.9; urbanized areas equal 0.8; industrial areas equal 0.7; agriculture equals 0.5; land covered with sparse vegetation equals 0.4; grass and parks equal 0.2; forests equal 0.1	

After standardization, it is necessary for decision-makers to define the significance factors of particular criteria using the appropriate coefficient weights (weights) or the criteria weights. The next section explains a method of determining the criteria weights presented in the studied case. As previously mentioned, the study involved 10 experts who carried out the expert evaluation criteria; see Table 3.

Table 3. Matrices of experts' comparison in theevaluation criteria pairs.

Expert 1						
	C1	**C2**	**C3**	**C4**	**C5**	**C6**
C1	(1.00;1.00)	(0.13;0.14)	(5;7)	(0.2;0.25)	(4;5)	(0.13;0.14)
C2	(8;7)	(1.00;1.00)	(9;9)	(2;3)	(9;9)	(1.00;1.00)
C3	(0.2;0.14)	(0.11;0.11)	(1.00;1.00)	(0.11;0.13)	(0.25;0.33)	(0.11;0.11)
C4	(5;4)	(0.5;0.33)	(9;8)	(1.00;1.00)	(7;8)	(0.25;0.33)
C5	(0.25;0.2)	(0.11;0.11)	(4;3)	(0.14;0.13)	(1.00;1.00)	(0.11;0.13)
C6	(8;7)	(1.00;1.00)	(9;9)	(4;3)	(9;8)	(1.00;1.00)
			...			
Expert 10						
	C1	**C2**	**C3**	**C4**	**C5**	**C6**
C1	(1.00;1.00)	(0.14;0.11)	(1.00;1.00)	(0.2;0.25)	(6;7)	(0.14;0.11)
C2	(7;9)	(1.00;1.00)	(7;8)	(3;4)	(9;9)	(1;2)
C3	(1.00;1.00)	(0.14;0.13)	(1.00;1.00)	(0.2;0.25)	(7;8)	(0.14;0.13)
C4	(5;4)	(0.33;0.25)	(5;4)	(1.00;1.00)	(9;8)	(0.33;0.25)
C5	(0.14;0.17)	(0.11;0.11)	(0.14;0.13)	(0.11;0.13)	(1.00;1.00)	(0.11;0.13)
C6	(7;9)	(1;0.5)	(7;8)	(3;4)	(9;8)	(1.00;1.00)

After filling in the matrix of comparisons in pairs (Table 3), we see that there is a definite dose of uncertainty when comparing the expert criteria. It is concluded on the basis of the values, which are given out by experts in the comparison matrices. Thus, at the position of C1–C5, in a comparison matrix DM1, the first expert entered two values ($z_{15} = 4$; $z'_{15} = 5$). This means that the expert could not choose one of the values four or five. If there is no uncertainty, then the expert e will undoubtedly select one value. An example of this is for the position of C2–C5 in the matrix DM1. The first expert introduced two same value in the comparison matrix DM1 ($z_{25} = 9$; $z'_{25} = 9$).

The consistency ratio for the comparison matrix is determined after the criteria comparison in pairs. Since the expert enters two values for each position in matrix Z_k, $(z^e_{ij}; z^{e\prime}_{ij})$, two consistency ratios are obtained for each expert CR^e and $CR^{e'}$. After calculating the consistency ratio for the comparison matrix (Table 4), it can be concluded that the research is valid, because all values $CR_e < 0.1$. Thus, e.g., for the first expert (Table 4), it is $CR_1 = (0.022 + 0.088)/2 = 0.055$.

Table 4. CR_e comparison matrix and experts' weights.

Expert	CR^e	$CR^{e'}$	CR^e	w_{ke}
E 1	0.022	0.088	0.055	0.102
E 2	0.071	0.087	0.079	0.071
E 3	0.035	0.064	0.049	0.114
E 4	0.081	0.067	0.074	0.076
E 5	0.022	0.051	0.036	0.155
E 6	0.083	0.067	0.075	0.075
E 7	0.037	0.071	0.054	0.105
E 8	0.031	0.065	0.048	0.118
E 9	0.044	0.057	0.050	0.112
E 10	0.092	0.067	0.079	0.071

In order to obtain an interval rough averaged comparison matrix, based on the data in Table 3 and using Expressions (1)–(13), the elements x_{ij}^e and $x_{ij}^{e\prime}$ of matrix X_k are transformed into interval rough number $IRN(z_{ij}^e)$. Thus, ten interval rough matrices are calculated X_k. Using Equations (22), (23) and experts' weight coefficients (Table 4), the average interval rough comparison matrix is calculated in evaluation criteria pairs; see Table 5.

Table 5. Interval rough average matrix.

	C1	C2	C3	...	C6
C1	([1.00,1.00],[1.00,1.00])	([0.59,4.41],[0.50,3.69])	([0.26,1.08],[0.26,1.34])		([0.29,1.84],[0.29,2.43])
C2	([0.27,1.89],[0.28,2.27])	([1.00,1.00],[1.00,1.00])	([4.79,6.87],[4.74,6.72])		([0.28,2.48],[0.36,2.77])
C3	([0.12,0.16],[0.13,0.19])	([0.31,2.06],[0.27,2.29])	([1.00,1.00],[1.00,1.00])		([1.23,6.30],[1.37,6.47])
C4	([4.79,6.87],[4.74,6.72])	([3.16,7.00],[3.82,7.13])	([6.36,8.31],[5.51,7.62])	...	([0.16,0.43],[0.15,0.32])
C5	([0.16,0.43],[0.15,0.32])	([0.72,5.73],[0.71,6.00])	([1.57,4.45],[1.42,4.86])		([0.41,4.01],[0.37,4.01])
C6	([0.25,1.63],[0.22,1.85])	([0.68,6.23],[0.65,5.88])	([1.04,5.02],[0.86,5.31])		([0.68,6.23],[0.65,5.88])
C7	([0.61,1.76],[0.45,1.41])	([1.67,6.96],[1.31,6.45])	([4.94,8.18],[4.36,7.69])		([1.00,1.00],[1.00,1.00])

Based on data from Table 5, and using Equations (25) and (26), the normalized matrix of weight coefficients W are calculated (Table 6.).

Table 6. Normalized matrix of weight coefficients.

	C1	C2	C3	...	C6
C1	([0.05,0.24],[0.04,0.26])	([0.02,0.09],[0.02,0.09])	([0.02,0.53],[0.02,0.45])		([0.01,0.51],[0.02,0.51])
C2	([0.06,0.3],[0.05,0.36])	([0.04,0.74],[0.04,0.94])	([0.02,0.69],[0.02,0.74])		([0.03,0.58],[0.04,0.73])
C3	([0.03,0.05],[0.03,0.06])	([0.02,0.06],[0.02,0.08])	([0.01,0.25],[0.01,0.28])		([0.01,0.11],[0.01,0.18])
C4	([0.16,0.4],[0.14,0.43])	([0.14,0.39],[0.14,0.42])	([0.09,0.85],[0.12,0.88])	...	([0.05,1.22],[0.06,1.27])
C5	([0.04,0.22],[0.04,0.27])	([0.02,0.17],[0.02,0.13])	([0.03,0.12],[0.03,0.12])		([0.02,0.78],[0.02,0.79])
C6	([0.06,0.31],[0.05,0.37])	([0.03,0.64],[0.03,0.77])	([0.02,0.75],[0.02,0.72])		([0.04,0.19],[0.04,0.2])
C7	([0.13,0.4],[0.11,0.43])	([0.08,0.69],[0.06,0.59])	([0.05,0.84],[0.04,0.79])		([0.05,1.08],[0.04,1.07])

Using (28), interval rough weight coefficients for evaluation criteria are obtained; see Table 7.

Table 7. Weight coefficients for evaluation criteria.

Criteria	Interval Rough Approach		Fuzzy Approach		Crisp Approach	
	$IRN(w_j)$	Rank	Fuzzy (w_j)	Rank	Crisp (w_j)	Rank
C1	([0.02,0.27],[0.02,0.3])	5	(0.08,0.12,0.16)	5	0.122	5
C2	([0.03,0.43],[0.04,0.5])	2	(0.11,0.19,0.21)	2	0.203	2
C4	([0.09,0.68],[0.09,0.7])	6	(0.04,0.08,0.07)	6	0.259	6
C5	([0.01,0.1],[0.01,0.12])	1	(0.25,0.32,0.55)	1	0.120	1
C6	([0.02,0.34],[0.02,0.35])	4	(0.07,0.14,0.15)	4	0.137	4
C7	([0.03,0.42],[0.03,0.43])	3	(0.12,0.15,0.19)	3	0.159	3

The process of weight criteria determining in this study was carried out in three scenarios in which, under the AHP arithmetic methods, different modalities' numbers are used (interval rough numbers, triangular fuzzy numbers and crisp value), with the aim of highlighting the most reliable modality.

The paired comparison criterion in fuzzy AHP methods was performed by applying the fuzzy scale with triangular fuzzy numbers; see Table 8 [93–96]. For the comparison in pairs of the traditional AHP method, the classic Saaty scale is used, in Table 8 [86].

Table 8. Saaty-etascale for comparison in pairs using fuzzy numbers.

Definition	Crisp Scale	Fuzzy Scale
Equal importance	1	(1,1,1)
Somewhat more important	3	(2,3,4)
Much more important	5	(4,5,6)
Very much more important	7	(6,7,8)
Absolutely more important	9	(8,9,9)
Intermediate values	2, 4, 6, 8	(x − 1, x, x + 1)

The most reliable modality has been confirmed by the validation process, which is presented in Section 5. Table 7 shows the interval rough weights and the values of coefficients, which are obtained by the traditional crisp AHP and fuzzy AHP (F'AHP) methods. When calculating the value weights using the F'AHP method, the symmetrical triangular fuzzy numbers form is used. From Table 7, it can be seen that all three methods of generating weight coefficient sequences are of the same rank (C5 > C2 > C7 > C6 > C1 > C4), but with different values.

4.3. Aggregation of Weighted Linear Combination

Weighted linear combination (WLC) method is used in the process of criteria map aggregation. In addition, it is compensatory, meaning that low scores in one criterion can be compensated by high scores in another one, which is desired for this particular decision problem. For these reasons, WLC was selected as the method of aggregation. The weighted linear combination (WLC) method multiplies each fuzzy standardized criteria map (i.e., each raster cell 15 m × 15 m) with criteria weights, obtaining different variations from the AHP method, and then sums the results. The mathematical expression for calculating the suitability index in the WLC is given as follows (28):

$$S = \sum w_i x_i \tag{28}$$

where S is the suitability index, w_i is the normalized value of the factor weight and x_i is the criterion score of factor i.

On the basis of the adopted criteria and the determination of their weight, according to the three scenarios described in the previous part, the WLC is used to execute the aggregation map of the criteria in the final flood hazard map, which is presented in the same fuzzy value range from 0 to 1.Finally, the flood hazard index is calculated using the defuzzification algorithm by the Standard Deviation method from the Reclass Spatial Analyst Tools ArcGIS 10.2 software release. Based on this, each cell is classified into five categories and receives a new value from 1 to 5 representing the flood hazard index (FHI).

The results of the urban flood hazard assessment are given in the maps of Figure 5. The maps were made according to three different scenarios using the AHP method. The first scenario exploits uncertainty using interval rough numbers in the AHP method (IR'AHP). The second uses the fuzzy technique method for exploiting of the uncertainty in the AHP (F'AHP), and the third scenario considers the use of the traditional (crisp) AHP method. The study area of each map was classified into five sections corresponding to very high, high, moderate, low and very low flood hazard zones. The percentages of these classes, in relation to the entire study area, are given in Table 9.

Table 9. The areas of classes from the final flood hazard map for the scenarios. IR, interval rough number; F, fuzzy.

Flood Hazard Index		Scenario 1 IR'AHP		Scenario 2 F'AHP		Scenario 3 Crisp AHP	
		(km^2)	%	(km^2)	%	(km^2)	%
FHI 5	Very high	12.9	18.5	8.8	12.6	7.8	11.2
FHI 4	High	16.2	23.2	20.7	29.6	24.9	35.6
FHI 3	Moderate	15.1	21.6	17.2	24.6	15.3	21.9
FHI 2	Low	8.5	12.2	14.7	21.0	12.2	17.5
FHI 1	Very low	17.2	24.6	8.5	12.2	9.7	13.9

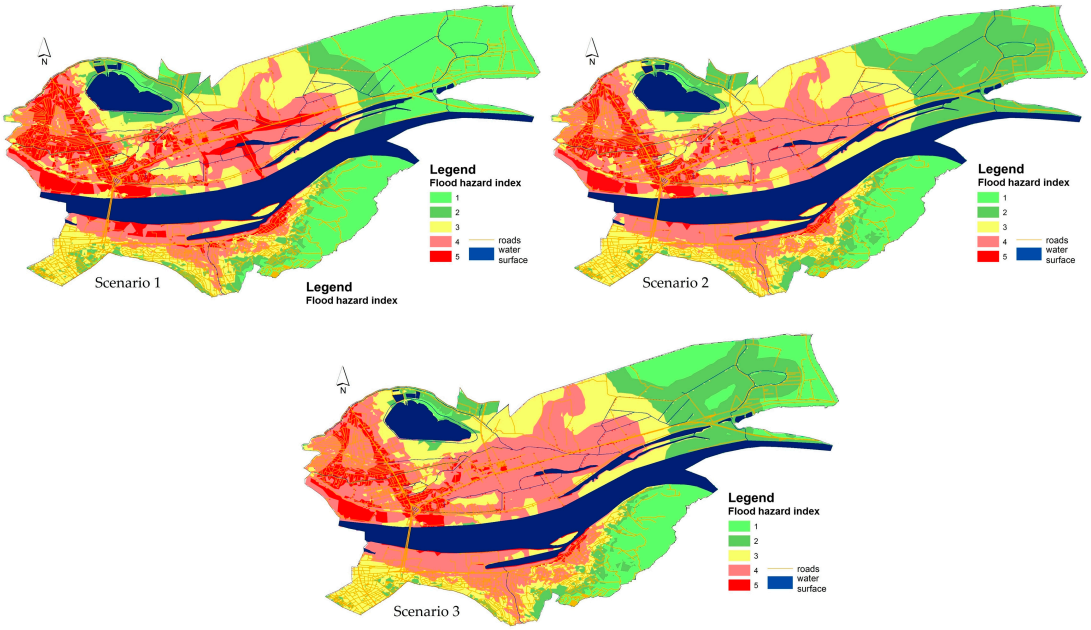

Figure 5. Final flood hazard maps for the scenarios.

Figure 5 displays the final flood risk maps obtained by the WLC aggregating method for three scenarios.

Statistical analysis of the results is obtained from the final flood risk maps (Table 9). According to Scenario 1, when applying the IR'AHP technique, very high surface areas (FHI 5) in Palilulaare 12.9 km^2, which is about 18.5% of the territory of the community. Under Scenario 2, which uses the fuzzy technique in the AHP method (F'AHP), the FHI 5 area is 8.8 km^2, while in Scenario 3, with the traditional (crisp) AHP method applied, the FHI 5 area is calculated to be 7.8 km^2 for the occurrence of floods. Spatially, all three maps shows that these are the parts on the left bank of the Danube, which gravitate towards the sewage network. At the same time, these are the most ecologically-sensitive parts in which uncontrolled floods can lead to catastrophic environmental and social consequences.

5. Results-Discussions

Validation of flood hazard maps was performed on the basis of historical flood events that have been recorded in the area of research. Data on many high waters and floods in the past have been gathered from all relevant stakeholders involved in flood protection: the Republic Hydro-meteorological Service, the Republic Water Directorate, public water companies and the competent authorities of Palilula. Some data, for flooding that occurred in 2010 and 2014, by the "Questionnaire on flood event", were collected directly in the field. In the period from 1938 to 2016, 31 major flood events were identified caused by spillover of the sewage network and the spill from the

bed of the channel and the river, mainly on the sections along which there are systems built for flood protection, but also on protected areas due to spill-over protective structures.

In Figure 6, the green circles show the locations of historical flood events. The majority of the city's historic flooding is located left, next to the Danube River, and in the urban part on the left bank of the Danube.

For the validation of the final results obtained by applying the GIS MCDA methodology for flood hazard assessment, it is necessary to determine the spatial relationship between the historical flooding sites and the flood hazard maps made. For the purposes of this analysis, we used the algorithm "Extract by Mask" integrated within the software environment ArcGis10.2. Based on this tool, the cell grid that corresponds to historically-flooded areas, based on the spatial coincidence, is extracted in one of five different levels of flood hazard, according to different scenarios. The results of this analysis are presented in Table 10.

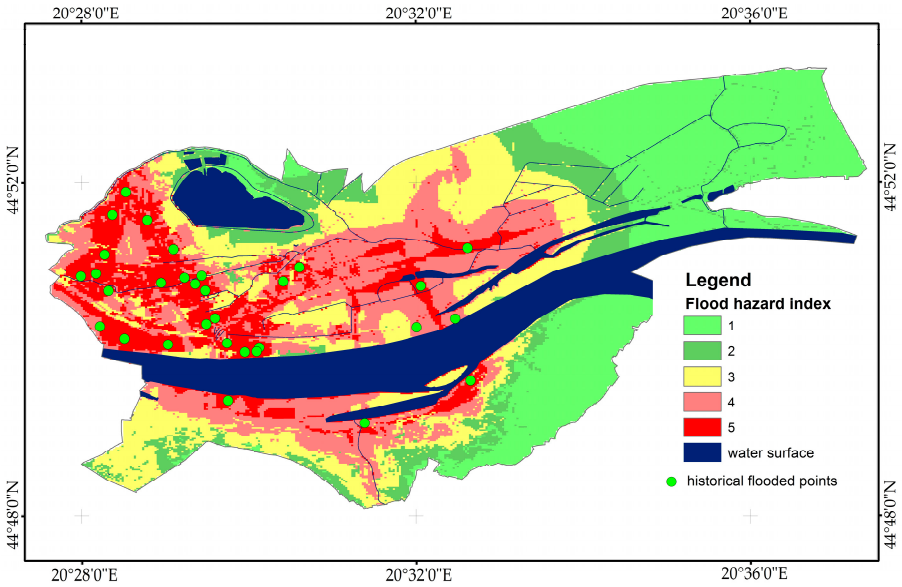

Figure 6. Validation of the final flood hazard map (IR'AHP) with historically-flooded points.

Table 10. Spatial relations of the historical floods locations and flood hazard zones according to the scenarios.

Scenarios	Historically-Flooded Points	Flood Hazard Index (FHI)				
		5	4	3	2	1
1 IR'AHP	31	27 (87.1%)	4 (12.9%)	0	0	0
2 F'AHP	31	21 (67.7%)	9 (29.0%)	1(3.2%)	0	0
3 AHP (crisp)	31	17 (54.8%)	10 (32.3%)	4 (12.9%)	0	0

Based on the validation results from Table 10, a relatively high consistency of the applied GIS-AHP methodology can be seen. The biggest consistency of historical flooding events of the final flood hazard map was drawn up on the basis of the IR'AHP method use, according to Scenario 1. Scenario 2 has been less consistent with the final flood risk map made using F'AHP. The least consistency has been shown using Scenario 3, in which the criteria weights were calculated using the traditional (crisp) AHP method.

Considering the flood hazard map in Scenario 1 (Figure 6), it can be seen that 27% or 87.1% of the recorded historical flood locations coincide with the zone of very high flooding hazard, while the four floods coincide with the zone of very high flooding hazard. In this way, the reliability of the proposed

methodology is confirmed, thus ensuring the certainty of the results of this analysis. Therefore, it can be concluded that the *IRN*'s use is justified in the process of determining the criteria weights, since the proposed IR'AHP methodology successfully exploited ambiguities and objectively reflects the perceptions of decision-makers.

Spatial analysis obtained by overlapping flood hazard zone maps with different thematic content maps can give general conclusions about the potential risk of flooding in Palilula. Table 11 shows the data of the exposure of certain land use and infrastructure elements according to the flooding hazard zones.

Table 11. The exposure to the flooding hazard in Palilula.

Land Cover/Infrastructure	Unit	Flood Hazard Index				
		5	**4**	**3**	**2**	**1**
Urban areas	km^2	7.85	6.42	3.90	12.84	0.57
Grassland	km^2	0.12	0.32	0.53	0.60	0.96
Forests	km^2	0.24	0.63	1.69	0.81	2.38
Scrub	km^2	0.17	0.29	0.31	0.18	0.12
Arable land	km^2	2.06	7.85	6.42	3.90	12.84
Industrial areas	km^2	0.34	0.99	0.45	0	0
Parks	km^2	0.009	0.45	0.086	0.107	0.003
Marshes	km^2	0.92	0.22	0.02	0	0
Schools and universities	No.	11	17	9	6	0
Kindergartens	No.	9	8	5	2	0
Residential buildings	No.	540	407	449	114	25
Industrial buildings	No.	11	13	6	0	0
Medical facilities	No.	4	1	1	0	0
Roads	km	36.77	38.54	32.30	16.94	20.80
Railroads	km	0.64	2.26	3.44	0.74	0.83
Population	thousands	41,565	31,108	18,568	11,540	7856

From Table 11, it can be seen that about 75 km of roads and 3 km of railways and 950 residential buildings with about 72,500 inhabitants are located in zones of high and very high flood hazard. Furthermore, this zone covers 15 km^2 of urban area. The general conclusion is that the risk of flood covers much of the demographic and infrastructural resources of Palilula municipality.

6. Conclusions

The paper tests the application of the GIS-IR'AHP modified methodology for zoning flood hazard in urban areas in the case of the Municipality of Palilula in Belgrade, Serbia. It is a methodology that can be applied to other sites with similar characteristics. The association of these tools is provided in the Advanced ArcGIS 10.2 software environment of the company ESRI. The methodology considers six factors that are relevant to the hazard of flooding in urban areas: the height, slope, distance to the sewage network, the distance from the water surface, the depth of groundwater and land use. The process of comparing and determining the weight criteria included three scenarios used under the AHP method: interval rough numbers, fuzzy numbers and crisp value. Final maps of areas of the hazard of flooding, according to different scenarios, were obtained using weighed linear combination (WLC). The validation of the results was carried out on the basis of comparison, an event of historic floods that were recorded in the area of research, with defined zones of hazard on the final maps.

Results of the validation show that Scenario 1 is the most consistent with the historical events of flooding. Based on these indicators, the authors propose an original approach for determining the weight criteria implementing the new methodology IR'AHP. The results of the GIS-IR'AHP methodology of Scenario 1 resulted in the final aggregation of risk maps of flood zones, the definition of the flood hazard index (FHI). They show that 12.9 km^2 or 18.5% of the Palilula municipality has a very high-hazard, the high-hazard area being 23.2% and 21.6% for moderate hazard with respect to the occurrence of flood events. On the other hand, 8.5 km^2 or 12.2% of the area has very low and 24.6%

has low hazard in the occurrence of floods. From these results, it is evident that Palilula municipality is mostly located in areas of high hazard with the probability of the occurrence of high water and flooding. These parts are mostly on the left bank of the Danube and parts that gravitate toward the sewage canal network of the community.

Application of GIS-IR'AHP in defining flood hazard zones in urban areas proved to be justified because it is based on the adopted criteria, with a high degree of reliability of the differentiated parts on the premises of a high-hazard of the occurrence of floods. The result is a mapping of flood hazard, which is the first step in the development of flood hazard management plans and determining areas where there is or might appear significant hazard of flooding, with harmful consequences for human health, the environment, economic activities and cultural heritage. In addition to the guidelines in water management, the application of the methodology can serve spatial planners to create a space policy in the area of urban land use plans and insurance companies for the evaluation of potential flood damage. The results of the work, in front of spatial planners and city government, impose the necessity to take austerity measures regarding uncontrolled urbanization, particularly in high-hazard areas near bodies of water and clogging city canal water. In addition, it is necessary to define new urban plan construction rules that require the increase of the permeable surface and the increase of the value of the runoff coefficient to surface runoff. Furthermore, one of the potentially good measures related to the collection and storm water drainage in the municipality of Palilula is to partially convert sewage into the general sewer separation system. However, only in places where it is close to the recipient and where it is estimated that the water will be too polluted, it does not have to go to the treatment plant prior to discharging to the recipient.

This study presents evidence of the importance and reliability of the application of the mixed GIS and MCDA technique in the assessment of phenomena that require expert opinion and manipulate a large number of data from different sources. The current issue discusses the new GIS-IR'AHP methodology, which creates the basis for further theoretical and practical upgrade. The present methodology allows the inclusion of new criteria that were not considered in the work, which are relevant to this issue (flow accumulation, flow direction, wetness index, rainfall, soil type, etc.). Furthermore, it is possible to use digital urban projects and large-scale orthophotos and satellite images with high spatial resolution, to provide detailed mapping of hazard zones in urban areas, which can improve the results. All of these factors may have an additional role in the upgrading of the present methodology and choosing the best solutions.

Acknowledgments: This work supported research project VA/TT/3/17-19 "GIS modeling of risk assessment of disasters and catastrophes in the function of the third mission of the Army of Serbia"by the Ministry of Defence of the Republic of Serbia.

Author Contributions: This research was carried out in collaboration between all authors. Ljubomir Gigović and Siniša Drobnjak designed this research and collected data. Dragan Pamučar and Zoran Bajić performed the simulation of the multi-criteria and the methodology. The discussions and analysis were carried out by all authors. All authors have read and approved the final manuscript.

Conflicts of Interest: The authors declare no conflict of interest.

Appendix A

Arithmetic operations between two *IRN* $IRN(A) = ([a_1, a_2], [a_3, a_4])$ and $IRN(B) = ([b_1, b_2], [b_3, b_4])$ are conducted using Equations (A1)–(A7):

(1) Adding of *IRN*"+"

$$IRN(A) + IRN(B) = ([a_1, a_2], [a_3, a_4]) + ([b_1, b_2], [b_3, b_4]) = ([a_1 + b_1, a_2 + b_2], [a_3 + b_3, a_4 + b_4]) \quad \text{(A1)}$$

(2) Subtraction of *IRN*"−"

$$IRN(A) - IRN(B) = ([a_1, a_2], [a_3, a_4]) - ([b_1, b_2], [b_3, b_4]) = ([a_1 - b_4, a_2 - b_3], [a_3 - b_2, a_4 - b_1]) \quad \text{(A2)}$$

(3) Multiplication of *IRN*"×"

$$IRN(A) \times IRN(B) = ([a_1, a_2], [a_3, a_4]) \times ([b_1, b_2], [b_3, b_4]) = ([a_1 \times b_1, a_2 \times b_2], [a_3 \times b_3, a_4 \times b_4]) \quad \text{(A3)}$$

(4) Dividing of *IRN*"/"

$$IRN(A)/IRN(B) = ([a_1, a_2], [a_3, a_4])/([b_1, b_2], [b_3, b_4]) = ([a_1/b_4, a_2/b_3], [a_3/b_2, a_4/b_1]) \quad \text{(A4)}$$

(5) Scalar multiplication of *IRN* where $k > 0$

$$k \times IRN(A) = k \times ([a_1, a_2], [a_3, a_4]) = ([k \times a_1, k \times a_2], [k \times a_3, k \times a_4]) \quad \text{(A5)}$$

Any IRN $IRN(\alpha) = \left(\left[\alpha^L, \alpha^U\right], \left[\alpha'^L, \alpha'^U\right]\right)$ i $IRN(\beta) = \left(\left[\beta^L, \beta^U\right], \left[\beta'^L, \beta'^U\right]\right)$ is ranked using these rules:

(1) If the intervals of *IRN* are not strictly bounded by other intervals, then:

- (a) If the condition is satisfied that $\{\alpha'^U > \beta'^U$ and $\alpha^L \geq \beta^L\}$ or $\{\alpha'^U \geq \beta'^U$ and $\alpha^L < \beta^L\}$, then $IRN(\alpha) > IRN(\beta)$; Figure A1a.
- (b) If the condition is satisfied that $\{\alpha'^U = \beta'^U$ and $\alpha^L = \beta^L\}$, then $IRN(\alpha) = IRN(\beta)$; Figure A1b.

(2) If the intervals of *IRN* $IRN(\alpha)$ and $IRN(\beta)$ are strictly bounded by other intervals, then it is necessary to find intersection points $I(\alpha)$ and $I(\beta)$ of *IRN* $IRN(\alpha)$ and $IRN(\beta)$. Then, if this is satisfied, $\beta'^U < \alpha'^U$ and $\beta^L > \alpha^L$.

- (a) If the condition is satisfied that $I(\alpha) \leq I(\beta)$, then $IRN(\alpha) < IRN(\beta)$; Figure A1c,d.
- (b) If the condition is satisfied that $I(\alpha) > I(\beta)$, then $IRN(\alpha) > IRN(\beta)$; Figure A1e.

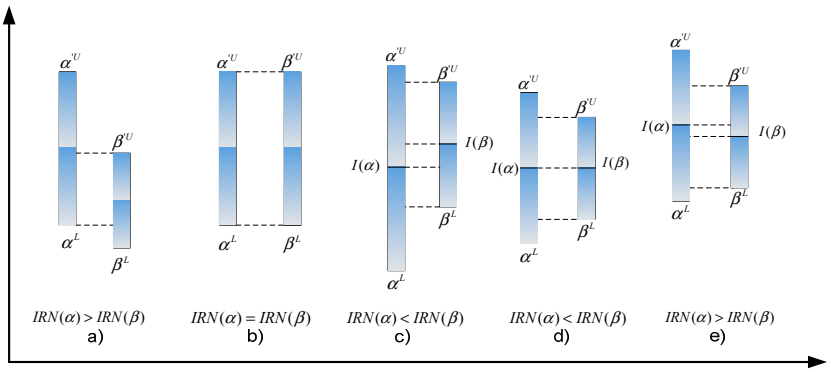

Figure A1. Ranking of interval rough numbers (*IRN*).

Intersection points for *IRN* are calculated as follows:

$$\mu_\alpha = \frac{RB(\alpha_{ui})}{RB(\alpha_{ui}) + RB(\alpha_{li})}; RB(\alpha_{ui}) = \alpha'^U - \alpha'^L; RB(\alpha_{li}) = \alpha^U - \alpha^L \quad \text{(A6)}$$

$$\mu_\beta = \frac{RB(\beta_{ui})}{RB(\beta_{ui}) + RB(\beta_{li})}; RB(\beta_{ui}) = \beta'^U - \beta'^L; RB(\beta_{li}) = \beta^U - \beta^L \quad \text{(A7)}$$

$$I(\alpha) = \mu_\alpha \cdot \alpha^L + (1 - \mu_\alpha) \cdot \alpha'^U \quad \text{(A8)}$$

$$I(\beta) = \mu_\beta \cdot \beta^L + (1 - \mu_\beta) \cdot \beta'^U \quad \text{(A9)}$$

References

1. Duan, W.; He, B.; Takara, K.; Luo, P.; Nover, D.; Yamashiki, Y.; Huang, W. Anomalous atmospheric events leading to Kyushu's flash floods, 11–14 July 2012. *Nat. Hazards* **2014**, *73*, 1255–1267. [CrossRef]
2. Aronica, G.T.; Brigandí, G.; Morey, N. Flash floods and debris flow in the city area of Messina, north-east part of Sicily, Italy in October 2009: The case of the Giampilieri catchment. *Nat. Hazards Earth Syst.* **2012**, *12*, 1295–1309. [CrossRef]
3. Forkuo, E.K. Flood Hazard Mapping using Aster Image data with GIS. *Int. J. Geomat. Geosci.* **2011**, *1*, 19.
4. Yahaya, S.; Ahmad, N.; Abdalla, R.F. Multi-criteria analysis for flood vulnerable areas in Hadejia-Jama'are River basin, Nigeria. *Eur. J. Sci. Res.* **2010**, *42*, 71–83.
5. Tsakiris, G. Flood risk assessment: Concepts, modelling, applications. *Nat. Hazards Earth Syst.* **2014**, *14*, 1361–1369. [CrossRef]
6. Chen, J.; Hill, A.A.; Urbano, L.D. A GIS-based model for urban flood inundation. *J. Hydrol.* **2009**, *373*, 184–192. [CrossRef]
7. Huong, H.T.L.; Pathirana, A. Urbanization and climate change impacts on future urban flooding in Can Tho city, Vietnam. *Hydrol. Earth Syst. Sci.* **2013**, *17*, 379–394. [CrossRef]
8. Sowmya, K.; John, C.M.; Shrivasthava, N.K. Urban flood vulnerability zoning of Cochin City, southwest coast of India, using remote sensing and GIS. *Nat. Hazards* **2015**, *75*, 1271–1286. [CrossRef]
9. Fernández, D.S.; Lutz, M.A. Urban flood hazard zoning in Tucumán Province, Argentina, using GIS and multicriteria decision analysis. *Eng. Geol.* **2010**, *111*, 90–98. [CrossRef]
10. Yang, W.; Sun, X.; Deng, W.; Zhang, C.; Liao, Q. Fourier Locally Linear Soft Constrained MACE for facial landmark localization. *CAAI Trans. Intell. Technol.* **2016**, *1*, 241–248. [CrossRef]
11. Brigandì, G.; Bonaccorso, B.; Aronica, G.T.; Gueli, R.; Basile, G. Flood and Landslide Warning based on rainfall thresholds and soil moisture indexes: The SyS Alert model for Sicily. In Proceedings of the 15th Risks Plinius Conference, Giardini Naxos, Italy, 8–11 June2016.
12. *Directive 2007/60/EC of the European Parliament and of the Council of 23 October 2007 on the Assessment and Management of Flood Risks*; Official Journal of the European Union L288 on 6.11.2007; European Union: Brussels, Belgium, 2007; pp. 27–34.
13. Büchele, B.; Kreibich, H.; Kron, A.; Thieken, A.; Ihringer, J.; Oberle, P.; Merz, B.; Nestmann, F. Flood-risk mapping: Contributions towards an enhanced assessment of extreme events and associated risks. *Nat. Hazards Earth Syst. Sci.* **2006**, *6*, 485–503. [CrossRef]
14. Zerger, A. Examining GIS decision utility for natural hazard risk modelling. *Environ. Model. Softw.* **2002**, *17*, 287–294. [CrossRef]
15. Wang, Y.; Li, Z.; Tang, Z.; Zeng, G. A GIS-based spatial multi-criteria approach for flood risk assessment in the Dongting Lake Region, Hunan, Central China. *Water Resour. Manag.* **2011**, *25*, 3465–3484. [CrossRef]
16. Vahidnia, M.H.; Alesheikh, A.A.; Alimohammadi, A.; Hosseinali, F. A GIS-based neurofuzzy procedure for integrating knowledge and data in landslide susceptibility mapping. *Comput. Geosci.* **2010**, *36*, 1101–1114. [CrossRef]
17. Patel, D.P.; Srivastava, P.K. Flood hazards mitigation analysis using remote sensing and GIS: Correspondence with town planning scheme. *Water Resour. Manag.* **2013**, *27*, 2353–2368. [CrossRef]
18. Jaafari, A.; Najafi, A.; Pourghasemi, H.R.; Rezaeian, J.; Sattarian, A. GIS-based frequency ratio and index of entropy models for landslide susceptibility assessment in the Caspian forest, northern Iran. *Int. J. Environ. Sci. Technol.* **2014**, *11*, 909–926. [CrossRef]
19. Strobl, R.O.; Forte, F.; Lonigro, T. Comparison of the feasibility of three flood-risk extent delineation techniques using Geographic Information System: Case study in Tavolieredelle Puglie, Italy. *Flood Risk Manag.* **2012**, *5*, 245–257. [CrossRef]
20. Gong, M.; Wang, S.; Liu, W.; Yan, J.; Jiao, L. Evolutionary computation in China: A literature survey. *CAAI Trans. Intell. Technol.* **2016**, *1*, 334–354. [CrossRef]
21. Pradhan, B.; Hagemann, U.; Tehrany, M.S.; Prechtel, N. An easy to use ArcMap based texture analysis program for extraction of flooded areas from TerraSAR-X satellite image. *Comput. Geosci.* **2014**, *63*, 34–43. [CrossRef]

22. Bathrellos, G.D.; Gaki-Papanastassiou, K.; Skilodimou, H.D.; Papanastassiou, D.; Chousianitis, K.G. Potential suitability for urban planning and industry development by using natural hazard maps and geological-geomorphological parameters. *Environ. Earth* **2012**, *66*, 537–548. [CrossRef]
23. Bathrellos, G.D.; Skilodimou, H.D.; Chousianitis, K.; Youssef, A.M.; Pradhan, B. Suitability estimation for urban development using multi-hazard assessment map. *Sci. Total Environ.* **2017**, *575*, 119–134. [CrossRef] [PubMed]
24. Tehrany, M.S.; Pradhan, B.; Jebur, M.N. Spatial prediction of flood susceptible areas using rule based decision tree (DT) and a novel ensemble bivariate and multivariate statistical models in GIS. *J. Hydrol.* **2013**, *504*, 69–79. [CrossRef]
25. Hammond, M.J.; Chen, A.S.; Djordjevic, S.; Butler, D.; Mark, O. Urban flood impact assessment: A stateoftheart review. *Urban Water J.* **2015**, *12*, 14–29. [CrossRef]
26. Djordjevic, S.; Vojinovic, Z.; Dawson, R.; Savic, D.A. Uncertainties in flood modelling in urban areas. In *Applied Uncertainty Analysis for Flood Risk Management*; World Scientific: Singapore, 2014; pp. 297–334.
27. Malczewski, J. GIS-based multicriteria decision analysis: A survey of the literature. *Int. J. Geogr. Inf. Sci.* **2006**, *20*, 703–726. [CrossRef]
28. Rahmati, O.; Zeinivand, H.; Besharat, M. Flood hazard zoning in Yasooj region, Iran, using GIS and multi-criteria decision analysis, Geomatics. *Nat. Hazards Risk* **2016**, *7*, 1000–1017. [CrossRef]
29. Gigović, L.; Pamučar, D.; Božanić, D.; Ljubojević, S. Application of the GIS-DANP-MABAC multi-criteria model for selecting the location of wind farms: A case study of Vojvodina. *Renew. Energy* **2017**, *103*, 501–521. [CrossRef]
30. Zhong, Q.B.; Chen, F. Trajectory planning for biped robot walking on uneven terrain—Taking stepping as an example. *CAAI Trans. Intell. Technol.* **2016**, *1*, 197–209. [CrossRef]
31. Gigović, L.; Pamučar, D.; Bajić, Z.; Milićević, M. The Combination of Expert Judgment and GIS-MAIRCA Analysis for the Selection of Sites for Ammunition Depots. *Sustainability* **2016**, *8*, 372. [CrossRef]
32. Gigović, L.; Pamučar, D.; Lukić, D.; Marković, S. Application of the GIS—Fuzzy DEMATEL MCDA model for ecotourism development site evaluation: A case study of "Dunavskiključ", Serbia. *Land Use Policy* **2016**, *58*, 348–365. [CrossRef]
33. Gerl, T.; Bochow, M.; Kreibich, H. Flood Damage Modeling on the Basis of Urban Structure Mapping Using High-Resolution Remote Sensing Data. *Water* **2014**, *6*, 2367–2393. [CrossRef]
34. Chau, V.N.; Holland, J.; Cassells, S.; Tuohy, M. Using GIS to map impacts upon agriculture from extreme floods in Vietnam. *Appl. Geogr.* **2013**, *41*, 65–74. [CrossRef]
35. Kazakis, N.; Kougias, I.; Patsialis, T. Assessment of flood hazard areas at a regional scale using an index-based approach and analytical hierarchy process: Application in Rhodope–Evros region Greece. *Sci. Total Environ.* **2015**, *538*, 555–563. [CrossRef] [PubMed]
36. Papaioannou, G.; Vasiliades, L.; Loukas, A. Multi-criteria analysis framework for potential flood prone areas mapping. *Water Resour. Manag.* **2015**, *29*, 399–418. [CrossRef]
37. Liu, Z.; Wang, W.; Jin, Q. Manifold alignment using discrete surface Ricci flow. *CAAI Trans. Intell. Technol.* **2016**, *1*, 285–292. [CrossRef]
38. Kannan, M.; Saranathan, E.; Anbalagan, R. Comparative analysis in GIS-based landslide hazard zonation—A case study in Bodi—BodimettuGhat section, Theni District, Tamil Nadu, India. *Arab. J. Geosci.* **2014**, *8*, 691–699. [CrossRef]
39. Kritikos, T.; Davies, T.R.H. GIS-based multi-criteria decision analysis for landslide susceptibility mapping at northern Evia, Greece. *Z. Dt. Ges. Geowiss.* **2011**, *162*, 421–434.
40. Meyer, V.; Scheuer, S.; Haase, D. A multicriteria approach for flood risk mapping exemplified at the Mulderiver, Germany. *Nat. Hazards* **2009**, *48*, 17–39. [CrossRef]
41. Tehrany, M.S.; Pradhan, B.; Mansor, S.; Ahmad, N. Flood susceptibility assessment using GIS-based support vector machine model with different kernel types. *Catena* **2015**, *125*, 91–101. [CrossRef]
42. Gong, M.; Li, H.; Jiang, X. A multi-objective optimization framework for ill-posed inverse problems. *CAAI Trans. Intell. Technol.* **2016**, *1*, 225–240. [CrossRef]
43. Pradhan, B. Flood susceptible mapping and risk area delineation using logistic regression, GIS and remote sensing. *J. Spat. Hydrol.* **2010**, *9*, 1–18.

44. Kia, M.B.; Pirasteh, S.; Pradhan, B.; Rodzi, M.A.; Sulaiman, W.N.A.; Moradi, A. An artificial neural network model for flood simulation using GIS: Johor River Basin, Malaysia. *Environ. Earth Sci.* **2012**, *67*, 251–264. [CrossRef]
45. Lohani, A.K.; Goel, N.K.; Bhatia, K.K.S. Improving real time flood forecasting using fuzzy inference system. *J. Hydrol.* **2014**, *509*, 25–41. [CrossRef]
46. Saaty, T.L. *The Analytic Hierarchy Process: Planning, Priority Setting, Resource Allocation*; McGraw-Hill: New York, NY, USA, 1980.
47. Chandio, I.A.; Matori, A.N.B.; Yusof, K.B.W.; Talpur, M.A.H.; Balogun, A.L.; Lawal, D.U. GIS-based analytic hierarchy process as a multicriteria decision analysis instrument: A review. *Arab. J. Geosci.* **2013**, *6*, 3059–3066. [CrossRef]
48. Siddayao, G.P.; Valdez, S.E.; Fernandez, P.L. Analytic hierarchy process (AHP) in spatial modeling for flood plain risk assessment. *Int. J. Mach. Learn. Comput.* **2014**, *4*, 450. [CrossRef]
49. Stefanidis, S.; Stathis, D. Assessment of flood hazard based on natural and anthropogenic factors using analytic hierarchy process (AHP). *Nat. Hazards* **2013**, *68*, 569–585. [CrossRef]
50. Chakraborty, A.; Joshi, P.K. Mapping disaster vulnerability in India using analytical hierarchy process. *Geomat. Nat. Hazards Risk* **2014**, *7*, 308–325. [CrossRef]
51. Pourghasemi, H.R.; Pradhan, B.; Gokceoglu, C. Application of fuzzy logic and analytical hierarchy process (AHP) to landslide susceptibility mapping at Haraz watershed, Iran. *Nat. Hazards* **2012**, *63*, 965–996. [CrossRef]
52. Liu, H.; Tang, H.; Xiao, W.; Guo, Z.Y.; Tian, L.; Gao, Y. Sequential Bag-of-Words model for human action classification. *CAAI Trans. Intell. Technol.* **2016**, *1*, 125–136. [CrossRef]
53. Rozos, D.; Bathrellos, G.D.; Skillodimou, H.D. Comparison of the implementation of rock engineering system and analytic hierarchy process methods, upon landslide susceptibility mapping, using GIS: A case study from the Eastern Achaia County of Peloponnesus, Greece. *Environ. Earth Sci.* **2011**, *63*, 49–63. [CrossRef]
54. Ouma, Y.O.; Tateishi, R. Urban Flood Vulnerability and Risk Mapping Using Integrated Multi-Parametric AHP and GIS: Methodological Overview and Case Study Assessment. *Water* **2014**, *6*, 1515–1545. [CrossRef]
55. Bathrellos, G.D.; Karymbalis, E.; Skilodimou, H.D.; Gaki-Papanastassiou, K.; Baltas, E.A. Urban flood hazard assessment in the basin of Athens Metropolitan city, Greece. *Environ. Earth Sci.* **2016**, *75*, 319. [CrossRef]
56. Liu, H.; Wang, C.; Gao, Y. Scene-adaptive hierarchical data association and depth-invariant part-based appearance model for in door multiple objects tracking. *CAAI Trans. Intell. Technol.* **2016**, *1*, 210–224. [CrossRef]
57. Moel, H.D.; Vliet, M.V.; Aerts, J.C.J.H. Evaluating the effect of flood damage-reducing measures: A case study of the unembanked area of Rotterdam, the Netherlands. *Reg. Environ. Chang.* **2014**, *14*, 895–908.
58. Zhu, G.N.; Hu, J.; Qi, J.; Gu, C.C.; Peng, J.H. An integrated AHP and VIKOR for design concept evaluation based on rough number. *Adv. Eng. Inform.* **2015**, *29*, 408–418. [CrossRef]
59. Song, W.; Ming, X.; Wu, Z. An integrated rough number-based approach to design concept evaluation under subjective environments. *J. Eng. Des.* **2013**, *24*, 320–341. [CrossRef]
60. Statistical Office of the Republic of Serbia. *2011 Census of Population, Households and Dwellings in the Republic of Serbia*; Book 20, Comparative overview of the number of population in 1948–2011. Data by settlements, Belgrade; Statistical Office of the Republic of Serbia: Krajevo, Serbia, 2014.
61. Republic Hydrometeorological Institute of Serbia. Available online: http://www.hidmet.gov.rs/ciril/meteorologija/klimatologija_padav_rezim.php (accessed on 24 January 2017).
62. Đorđević, V.S. Temperature and Precipitation Trends in Belgrade and Indicators of Changing Extremes for Serbia. *Geogr. Pannon.* **2008**, *12*, 62–68.
63. Unkašević, M.; Tošić, I. A statistical analysis of the daily precipitation over Serbia: Trends and indices. *Theor. Appl. Climatol.* **2011**, *106*, 69–78. [CrossRef]
64. Zeshui, X.; Qingli, D. The possibility of interval number sequence method and its application. *J. Syst. Eng.* **2003**, *18*, 67–70.
65. Shuping, W. Interval multi-attribute decision-making of attitude indicator method. *Control Decis. Mak.* **2009**, *24*, 35–38.
66. Zadeh, L.A. Fuzzy sets. *Inf. Control* **1965**, *8*, 338–353. [CrossRef]
67. Xu, X.; Law, R.; Chen, W.; Tang, L. Forecasting tourism demand by extracting fuzzy Takagi-Sugeno rules from trained SVMs. *CAAI Trans. Intell. Technol.* **2016**, *1*, 30–42. [CrossRef]

68. Pamučar, D.; Ćirović, G. The selection of transport and handling resources in logistics centres using Multi-Attributive Border Approximation area Comparison (MABAC). *Expert Syst. Appl.* **2015**, *42*, 3016–3028. [CrossRef]
69. Song, W.; Ming, X.; Wu, Z.; Zhu, B. A rough TOPSIS approach for failure mode and effects analysis in uncertain environments. *Qual. Reliab. Eng. Int.* **2014**, *30*, 473–486. [CrossRef]
70. Zhang, Q.; Xie, Q.; Wang, G. A survey on rough set theory and its applications. *CAAI Trans. Intell. Technol.* **2016**, *1*, 323–333. [CrossRef]
71. Arce, M.E.; Saavedra, A.; Míguez, J.L.; Granada, E. The use of grey-based methods in multi-criteria decision analysis for the evaluation of sustainable energy systems: A review. *Sustain. Energy Rev.* **2015**, *47*, 924–932. [CrossRef]
72. Ji, W.; Tang, L.; Li, D.; Yang, W.; Liao, Q. Video-based construction vehicles detection and its application in intelligent monitoring system. *CAAI Trans. Intell. Technol.* **2016**, *1*, 162–172. [CrossRef]
73. Kuang, H.; Kilgour, D.M.; Hipel, K.W. Grey-based PROMETHEE II with application to evaluation of source water protection strategies. *Inf. Sci.* **2015**, *294*, 376–389. [CrossRef]
74. Vahdani, B.; Tavakkoli-Moghaddam, R.; Meysam, M.S. Soft computing based on new interval-valued fuzzy modified multi-criteria decision-making method. *Appl. Soft Comput.* **2013**, *13*, 165–172. [CrossRef]
75. Sizong, G.; Tao, S. Interval-Valued Fuzzy Number and Its Expression Based on Structured Element. *Adv. Intell. Soft Comput.* **2016**, *62*, 1417–1425.
76. Zywica, P.; Stachowiak, A.; Wygralak, M. An algorithmic study of relative cardinalities for interval-valued fuzzy sets. *Fuzzy Sets Syst.* **2016**, *294*, 105–124. [CrossRef]
77. Nayagama, V.L.G.; Jeevaraja, S.; Sivaraman, G. Complete Ranking of Intuitionistic Fuzzy Numbers. *Fuzzy Inf. Eng.* **2016**, *8*, 237–254.
78. Wang, H.; Yang, B.; Chen, W. Unknown constrained mechanisms operation based on dynamic interactive control. *CAAI Trans. Intell. Technol.* **2016**, *1*, 259–271. [CrossRef]
79. Nguyen, H. A new interval-value d knowledge measure for interval-valued intuitionistic fuzzy sets and application in decision making. *Expert Syst. Appl.* **2016**, *56*, 143–155. [CrossRef]
80. Zheng, P.; Xu, X.; Xie, S.Q. A weighted interval rough number based method to determine relative importance ratings of customer requirements in QFD product planning. *J. Intell. Manuf.* **2016**, 1–14. [CrossRef]
81. Kang, R.; Zhang, T.; Tang, H.; Zhao, W. Adaptive Region Boosting method with biased entropy for path planning in changing environment. *CAAI Trans. Intell. Technol.* **2016**, *1*, 179–188. [CrossRef]
82. Pawlak, Z. Rough sets. *Int. J. Comput. Inf. Sci.* **1982**, *11*, 341–356. [CrossRef]
83. Duntsch, I.; Gediga, G. The rough set engine GROBIAN. In Proceedings of the 15th IMACS World Congress, Berlin, Germany, 24–29 August 1997; Sydow, A., Ed.; Wissenschaft und Technik Verlag: Berlin, Germany, 1997.; Volume 4, pp. 613–618.
84. Khoo, L.P.; Zhai, L.Y. A prototype genetic algorithm enhanced rough set-based rule induction system. *Comput. Ind.* **2001**, *46*, 95–106. [CrossRef]
85. Saaty, T.L.; Vargas, L.G. *Models, Methods, Concepts and Applications of the Analytic Hierarchy Process*; Springer Science and Business, Media: Berlin, Germany, 2012.
86. Saaty, T.L. A scaling method for priorities in hierarchical structures. *J. Math. Psychol.* **1977**, *15*, 234–281. [CrossRef]
87. Stieglitz, M.; Rind, D.; Famiglietti, J.; Rosenzweig, C. An efficient approach to modeling the topographic control of surface hydrology for regional and global climate modeling. *J. Clim.* **1997**, *10*, 118–137. [CrossRef]
88. Youssef, A.M.; Pradhan, B.; Hassan, A.M. Flash flood risk estimation along the St. Katherine road, southern Sinai, Egypt using GIS based morphometry and satellite imagery. *Environ. Earth Sci.* **2011**, *62*, 611–623. [CrossRef]
89. Regmi, N.R.; Giardino, J.R.; Vitek, J.D. Modeling susceptibility to landslides using the weight of evidence approach: Western Colorado, USA. *Geomorphology* **2010**, *115*, 172–187. [CrossRef]
90. Glenn, E.; Morino, K.; Nagler, P.; Murray, R.; Pearlstein, S.; Hultine, K. Roles of *Saltcedar* (*Tamarix* spp.) and capillary rise in salinizing a non-flooding terrace on a flow-regulated desert river. *J. Arid Environ.* **2012**, *79*, 56–65. [CrossRef]
91. Kourgialas, N.N.; Karatzas, G.P. A flood risk decision making approach for Mediterranean tree crops using GIS; climate change effects and flood-tolerant species. *Environ. Sci. Policy* **2016**, *63*, 132–142. [CrossRef]

92. OpenStreetMap. Available online: https://www.openstreetmap.org/#map=11/44.9123/20.5197 (accessed on 27 January 2017).
93. Retaei, J.; Fahim, P.B.M.; Tavasszy, L. Supplier selection in the airline retail industry using a funnel methodology: Conjunctive screening method and fuzzy AHP. *Expert Syst. Appl.* **2014**, *41*, 8165–8179.
94. John, A.; Paraskevadakis, D.; Bury, A.; Yang, Z.; Riahi, R. An integrated fuzzy risk assessment for seaport operations. *Saf. Sci.* **2014**, *68*, 180–194. [CrossRef]
95. BalBeşikçi, E.; Kececi, T.; Arslan, O.; Turan, O. An application of fuzzy-AHP to ship operational energy efficiency measures. *Ocean Eng.* **2016**, *121*, 392–402. [CrossRef]
96. Aşchilean, I.; Badea, G.; Giurca, I.; Naghiu, G.S.; Iloaie, F.G. Choosing the optimal technology to rehabilitate the pipes in water distribution systems using the AHP method. *Energy Procedia* **2017**, *112*, 19–26. [CrossRef]